Richard Hofmeister

Model studies on stratification in the Limfjord

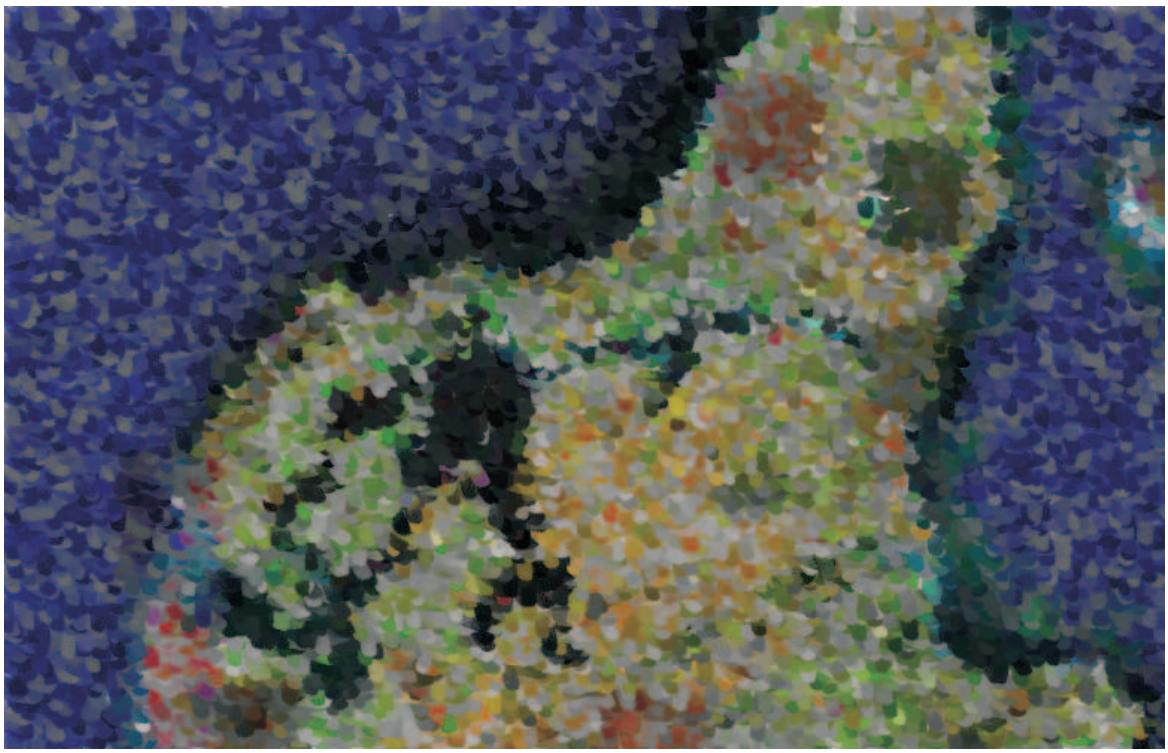

INSTITUT FÜR
OSTSEEFORSCHUNG
WARNEMÜNDE

Master Thesis

Section: Physical Oceanography and Instrumentation
Tutor: Prof. Dr. Hans Burchard

Contents

1 Motivation

In shallow seas and estuaries, understanding the physical effects of development and breakdown of stratification is a key to understand the ecosystem dynamics of such regions. Physical processes due to vertical mixing like heat flux, freshwater flux and momentum flux are controlled by the intensity of stratification. Biological properties in stratified waters depending on vertical mixing, like flux of nutrients, are suppressed and feed back on physical processes like absorption of solar radiation. For example, the primary production of phytoplankton takes place in a near-surface layer. Turbulent mixing disposes the produced phytoplankton in the water column. But in a stratified regime, suppressed turbulence at the pycnocline leads to a higher opacity, that means higher absorption rates in the mixing layer than in a well-mixed regime, when the plankton are displaced over the whole water column. Hence stratification is a fundamental control on primary production (*Sverdrup* [1953]).

Stratification and mixing does not only control primary production, but can have a large impact on the supply of phytoplankton to benthic filter feeders (*Frechette and Bourget* [1985]). In areas with high density of benthic filter feeders, like the Limfjord where mussels are grown on shellfish beds, the mussels can consume more phytoplankton than is transported downwards, which results in a depletion boundary layer near the sea bed (*Ackermann et al.* [2001],*Muschenheim and Newell* [1992]).

In periods of strong stratification or less mixing in the Limfjord the heavy bottom layer is decoupled from the upper layer. Then, the pycnocline prevents fluxes of nutrients, oxygen and phytoplankton, which can only come from the sea surface above, and the boundary depletion layer cannot be replenished. The mussel growth is reduced during these periods of food depletion, and in extreme cases of oxygen depletion the mussels will die.

The EU-Project MaBenE (short for: Managing Benthic Ecosystems in relation to Physical Forcing and Environmental constraints) started in 2002 and finished a short time ago in January 2006. Its aim was to study the physical and ecological regime in several mussel growth areas in Europe, including the Limfjord, in order to optimise shellfish production in terms of yield as well as nature conservation. In order to obtain a complete and realistic picture of the physical processes in the Limfjord, determining its benthic life, a realistic 3D-model was set up to study stratification and physical processes in the Limfjord. This thesis aims to report on these model studies and its results.

2 Stratification in the Limfjord

2.1 About the Limfjord

The Limfjord is a shallow sound in Denmark separating the Jutland Peninsula from the island Vendsyssel-Thy. It stretches from the Thyborøn channel (Figure 39 in the appendix shows a map) at the North Sea to Hals at Kattegat with a length of approximately 180 km. The name "Limfjord" is assumed to come from earlier times before 1825, when the Limfjord was only an estuary reaching from the only opening Kattegat into the Jutland Peninsula. On 3 February, 1825, the Limfjord was first opened to the North Sea side by a flood, building the so-called Agger-Canal. In 1862, another flooding created another opening in the remaining western boundary, called Thyborøn channel. In the late 19th century, the Agger-Canal was closed by continuous accumulation of sand.

The Limfjord is of irregularly shape with several bays, narrowings and islands. The connection to the North Sea is the Thyborøn channel, which leads into the western basin Nissum Bredning. A thin channel, called Oddesund, connects Nissum Bredning with the inner Limfjord which is dominated by islands and peninsulas, forming channels and bays. The island Mors in the western part of the inner Limfjord divides the Limfjord into two channels: Salling Sund, which carries the main flow and Nassund/Vilsund into a basin called Thisted Bredning. In the centre of the Limfjord is a shallow and wide basin called Løgstør Bredning. There is an estuary to the south with Risgårde Bredning connected via Hvalpsund to Skive Fjord and Lovns Bredning. To the east, Løgstør Bredning is connected to the Kattegat through a river-like channel, being connected to Kattegat at Hals. The main port of the Limfjord is Ålborg, where a railway and road bridge passes the Limfjord from Ålborg to Nørresundby.

The mean water depth is about 4.5 m and the deepest point is in Hvalpsund with a depth of 24 m. In Løgstør Bredning, the mean depth is about 5.8 m. There is a permanent horizontal salinity gradient between the two boundaries, having a salinity of 32-34 PSU at Thyborøn channel and 19-25 PSU at Hals. The total water volume in the Limfjord is 7.1 km^3, comparing to the net west-east throughflow of 8.7 km^3. That results in a residence time of 225 days (*Dame and Prins* [1998]). With a freshwater input from rivers in the same order of magnitude cumulating up to 2.4 km^3 in 2003, the Limfjord is neither controlled only by North Sea water, nor only by riverine freshwater, but rather by the interaction of both. The salinity in the inner parts of the Limfjord raise by 2 to 4 PSU over the whole year 2003. There were four major inflow events from the north sea side at the end of June, at the end of August, in October and an inflow at the very end of the year at the end of December. Temperature raise up to 20 degree Celsius during summer. In the winter period, the Limfjord is partially covered with ice. The regional wind field is dominated by westerly winds, building a higher sea surface elevation at the western boundary, than in the Kattegat boundary.

The Limfjord is famous for its tasty blue mussels (*Mytilus edulis*). The mussels

are said to have an extraordinary size and quality. The meat of the *Mytilus edulis* mussel meat is even available in popular supermarkets in Germany, but they are sold as North-Atlantic fjord mussels from the Limfjord. In the mussel fishery, the mussel beds are placed in the northern part of Løgstør Bredning at a depth of about 7.5 m at the sea bed. Future plans include the idea of growing the mussels on ropes attached to rafts. The advantage is that the mussels are near the primary production area at the surface and that they are not as endangered in times of stratification. About 100.000 t mussels are being harvested in the Limfjord per year (*Royal-Frysk* [2006]).

2.2 Production of stratification

2.2.1 Solar heating

In the open ocean, solar heating is the most important stratifying force. The parts of solar radiation which penetrate the sea surface without being reflected and sent back into the atmosphere immediately, react with the water molecules and particles in the water. This reaction is called absorption, and it depends on the spectrum and intensity of the incoming radiation and the degree of absorption, depending on the composition of the water including particles in it. The absorption can be parameterised by an exponential law of the intensity of radiation depending on the distance from the surface d.

$$I(d) = I_0 \cdot e^{-\frac{d}{g}} \tag{1}$$

with g as e-folding length, depending on the wavelength and I_0 as albedo-corrected surface radiation. The influence of radiation decreases exponentially, which means that in a depth of $z = 4.6 \times g$, the intensity of radiation equals approximately 1% of the intensity of radation at the surface. The range of the absorption length for visible light measures about two orders of magnitude from several 10 cm in dirty waters up to several 10 m in the open ocean.

In shallow areas and estuaries, the water temperature is not the most important agent in determining the stratification. In estuaries, fresh water from the river inflow is confronted with oceanic water with a relatively high salinity. The differences in salinity are of orders of magnitude, reaching from 0 PSU directly in the river water up to 35 PSU in the ocean. In shallow waters with a water depth, which equals approximately the absorption length, the solar radiation has an influence on the whole water column. In very shallow waters, there is a significant amount of radiation at the sea bed which is partially being reflected into the water column again. The residual radiation heats up the sea bed, resulting a heat flux from the sea bed into the near sea bed water. Furthermore, convective motions and wind stirring (see section 2.3) can mix the whole water column. Especially wind stirring of the whole water column results in increased temperatures even at the sea bed.

The Limfjord is a shallow estuarine area, such that is expected that saline stratification, due to mean horizontal gradients and freshwater supply, plays a more dominant role than thermal stratification, due to solar heating.

2.2.2 Precipitation

Another agent for stratification is precipitation. The fresh water from precipitation reaches the sea surface and wind induced turbulence mixes the fresh water with saline sea water. One can assume that the concentration of salt in the wind-mixed layer will decrease proportionally to the volume of fresh water from precipitation.

2.2.3 Differential advection

The total derivative of the water's density ρ may be formulated as the sum of local tendency by mixing, solar heating, evaporation or precipitation and the advection:

$$\frac{d\rho}{dt} = \frac{\partial \rho}{\partial t} + \vec{v} \cdot \vec{\nabla} \rho \tag{2}$$

with $\vec{v}$ being the flow velocity. When there is no gradient in direction of flow, there is no advective change in density. In natural waters like the Limfjord, advection is determined by the horizontal flow, so the gradient in density within the advective term has to have a horizontal part to cause an advective change. In this case, horizontal density gradients are typical for density fronts, which are the boundaries between stratified and well-mixed regimes. When stratification should increase because of advection, vertical inhomogeneities in either flow velocity or density gradients have to occur. The advection term then can be seen as a vertically inhomogeneous advective change which means that different advective changes occur in different water depths, the so called differential advection. The first case of the stratifying effect of differential advection is, that there is a vertically constant flow velocity over the whole water column, which advects a stratified regime from neighbouring water columns. In figure 1, this situation is shown in situation B. The vertical differences in the advection term in (2) are caused by vertical differences in the density gradient. The second case for the stratifying effect of differential advection is a current shear at density fronts. When there are no vertical differences in the density gradient, but a horizontal density gradient exists, vertical differences in density can be produced by vertical differences in velocity. In nature, this procedure occurs in tidally driven, shallow estuaries, called tidal straining. Substantial horizontal gradients of density are induced by freshwater input from rivers in estuaries. Initially, the isolines of salinity are vertically distorted by differential displacement. At ebb tide with a seaward flow, bottom friction induces a shear in currents. The surface water moves faster than the water near the sea bed and lets the light riverine water overtake the heavier, more saline water. A stable vertical structure is induced and sharpened by mixing effects by windstress and bottom shear. The mechanism is illustrated in Figure 2, taken from *Simpson et al.* [1990].

Estuarine circulation in general is determined by differential advection. With having horizontal gradients in density, an internal pressure gradient, which increases with depth, is produced by a higher hydrostatic pressure in areas with high density than in areas with lower density. It follows a flow from areas of higher density

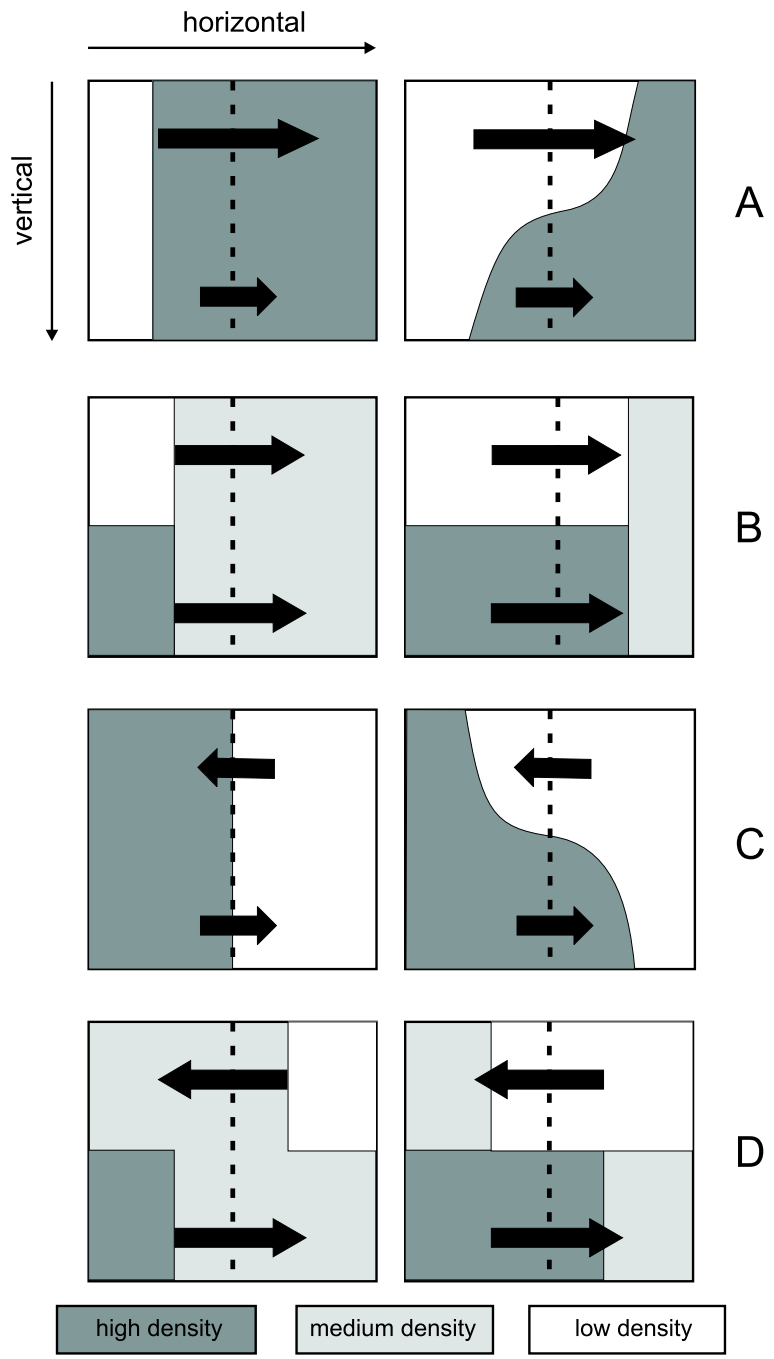

Figure 1: Four situations of stratifying. A&C: current shear and horizontal density gradient, B: advection of a stratified situation, D: differential advection The situations pictured on the left precede the situations on the right.

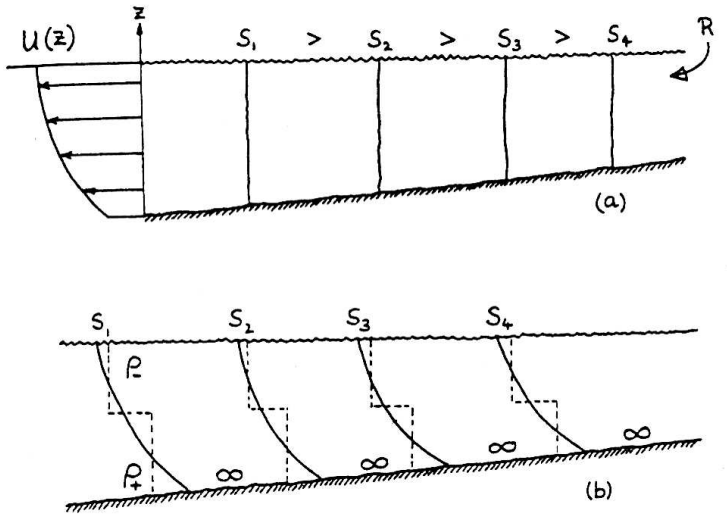

Figure 2: Schematic of tidal straining: (a) isolines vertical at start of ebb, (b) stratification induced by shear on the ebb modified by top and bottom mixing (picture taken from *Simpson et al.* [1990])

(mainly at the sea bed) to areas of lower density. The lighter, by the bottom flow lifted water flows backwards from areas of lower density to areas of higher density, driven by an elevation induced pressure gradient at the sea surface. The prototype of this circulation is the lock exchange. With removing an interface between water of high density and water of lower density, a stratifying circulation that was described above sets in. Figure 3 shows a simulated lock exchange with the 3D circulation model GETM some time after removing the interface between two water masses with a density difference of 5 kg m^{-3} in a closed rectangular basin, which is 64 km long and 20 m deep (see *Haidvogel and Beckmann* [1999]). The corresponding situation in Figure 1 is situation C. The principles of the lock exchange circulation and estuarine circulation are the same, but with the difference, that the estuarine system has a smooth horizontal gradient instead of a step in gradient like with the lock exchange system.

2.3 Destruction of stratification

In relation to stratification, a water column can have three principle states. One of these states is the fully mixed water column, that means homogeneous conditions in density ρ, depending on pressure, salinity and temperature. The stratified states are stable stratification and unstable stratification. Unstable stratification means that heavier water volumes lie above lighter water volumes. So it is an unsteady state of the water column, because as soon as there is denser water above lighter water, turbulence makes for mixing, so that the water becomes denser with depth. Stable

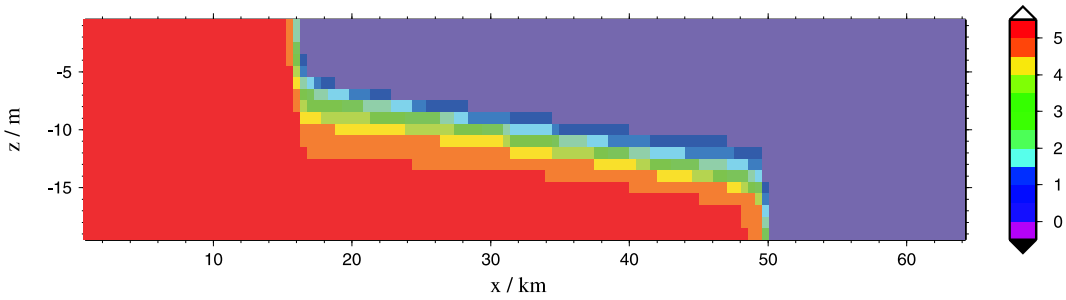

Figure 3: Density distribution in a lock-exchange model experiment, simulated with GETM.

stratification is the steady state being called "stratification" for simplicity. In this case, density increases with depth somehow, that means the dense water remains at the sea bed. Effects which destruct stratification have in common that turbulence is produced, resulting in vertical transports. Such physical effects are bottom shear driven by near-bed flow, surface shear by wind and unstable stratification by differential advection and surface cooling, including evaporation.

2.3.1 Surface shear

Wind can stir water bodies of any type. When one blows over the surface of coffee in a cup, waves occur and the water or coffee in the cup starts moving. The same effect is acting on oceanic waters. The wind blowing over oceanic water does not only slip over the water, but it causes stress on the sea surface and is towing the surface water in its direction. The momentum of surface water is transferred onto deeper layers by turbulent friction. Because these oceanic waters are located on a rotating earth, the Coriolis force causes every moving water volume to be diverted to the right hand side at the northern hemisphere and to be diverted to the left hand side at the southern hemisphere. The wind stress at the surface is proportional to the wind speed squared and gives a force per area.

$$\tau = C_d \cdot \rho_a \cdot v_{wind}^2$$

with C_d being the drag coefficient, ρ_a is the density of air and v_{wind} is the absolute wind velocity. This force drives a current on the surface and produces a shear in currents compared with lower layers. This shear produces turbulence that mixes the water column. The turbulent friction is assumed by parameterising turbulence statistically with the eddy viscosity and the vertical shear. This assumption was first formulated by Boussinesq. So the stress τ_{ij} being imposed from vertical layer i upon layer j is parameterised by

$$\tau_{ij} = \rho \cdot \nu_t \cdot S_{ij}$$

with ρ denoting the mean water density, ν_t being the eddy viscosity and $S_{ij} = (\partial_z u)_{i,j}$ being the shear in currents. Turbulence does not only cause turbulent fric-

tion, but it results in turbulent diffusion being parameterised statistically by a quantity called eddy diffusivity. Giving a turbulent flux of $\nu_t' \partial_z c$, with ν_t' being the eddy diffusivity and c being a scalar value such as potential temperature or salinity.

2.3.2 Bottom shear

Directly at the sea bed, the flow velocity equals zero because of adhesion at the sea bed. With a flow above, there is a shear in currents that produces turbulence similar to surface shear by wind stress at the sea surface. At the bottom, the force acting on the moving water volume by turbulent friction can be estimated with a stress $\tau_b = \rho(u^*)^2$ calculated from the density of water and the turbulent velocity scale u^*. The velocities outside the near-bed viscous layer can be described by a logarithmic law. It assumes that the effective roughness length at the bottom, z_0, is much smaller than the distance from the bottom:

$$\frac{u(z)}{u_*} = \frac{1}{\kappa} \cdot \ln\left(\frac{z}{z_0}\right) \tag{3}$$

where $\kappa \approx 0.41$ is the Karman constant and z is the distance from the bed. However, extrapolation of 3 to $z \to z_0$ results in $u(z_0) = 0$, i.e. zero velocity at the bed, such that the log-law down to the bed gives a sufficient parametrisation for the flows.

2.3.3 Surface cooling

Surface cooling is an effect that occurs mainly at night, when the water temperature is higher than the air temperature and when cold or dry winds are blowing over the sea surface. In both cases, heat flux from the surface water into the air cools down the surface water. The heat flux consists of the longwave back-radiation from the water, the sensible heat flux and the latent heat flux.

$$Q_{HF} = Q_s + Q_i + Q_l$$

The longwave back-radiation is black body radiation $Q_i \sim \sigma T^4$ with correction terms. These are needed, because the water body is not a black body and the emitted infrared radiation is absorbed by water vapour, carbon dioxide and greenhouse gases. These gases re-emit the infrared radiation into the ocean. Driven by the temperature difference between sea surface water and air, a sensible heat flux heats up the air at the sea surface. Even more than the sensible heat flux, the latent heat flux by evaporation cools down the sea surface.

When there are dry winds with a low relative humidity, water from the sea surface evaporates and takes the necessary amount of heat from the surface water. When there are cold winds that advect cold air or the air cools off at night, the sensible heat flux cools the surface water.

Surface cooling makes the surface water become denser than the water below. Therefore, vertical convection starts in the water column driven by the buoyancy

that forces the lighter water directed to the surface and gravitation that forces the relatively heavier water at the surface in the direction of the sea bed. This convective motion mixes the water column.

2.3.4 Destruction of stratification by differential advection

As already discussed in section 2.2.3, differential advection can produce stratification in an ebb tide regime with vertically isolines of density, but a horizontal density gradient, induced by estuarine freshwater input. In a high tide regime, the process of tidal straining in section 2.2.3 reverts and in a landward flow, bottom friction induces a shear in currents. The surface water moves faster than the water near the sea bed and lets the saline and thus heavy water overtake the lighter water and induces an instably stratified system. Convection mixes the watercolumn immediately.

2.4 Quantifying Stratification

When one wants to find results concerning stratification in the model, quantities describing stratification have to be considered. Obviously, stratification means that the density of water increases with water depth. A first way to estimate stratification is to calculate the difference between sea surface density and the water density at the sea bed.

$$\Delta\rho = \rho_{seabed} - \rho_{sea\ surface}$$

The sign and magnitude of this difference gives the type of stratification and a kind of an order of magnitude of stratification. By using the water depth H, a mean gradient can be calculated for each point in the considered waters - especially from this thesis' point of view in the Limfjord by

$$\overline{\left(\frac{\partial\rho}{\partial z}\right)} = \frac{\Delta\rho}{H}.$$

A constant density gradient in the whole water column is a very special case in natural waters. In general, a mixed layer at the sea surface and a mixed layer at the sea bed exists, because of shear produced turbulence at the sea bed and the surface and thermal convection at the surface like described in section 2.3. The gradient in density therefore is located vertically mainly between the bottom and surface mixed layer in the pycnocline, thus having a stronger magnitude than the mean gradient for the whole water column. Considering stratification and its production and destruction only by looking at density gradients as sole quantities is too simple. One has to take a look at energies, especially potential energy as quantity for energy stored in stratification and turbulent kinetic energy as an agent acting against this. The kinetic energy of a stratified flow does not primarily decrease stratification, only the turbulent kinetic energy, stored in turbulence, produced by a shear in currents, has an effect of mixing. When taking the equation for turbulent kinetic energy k in

a simple form

$$\frac{D}{Dt}k = -T + P + B - \varepsilon \tag{4}$$

with T being the transport, P is the shear production, B is the buoyant production and ε is the dissipation. The left hand side is the total deviation in time for the turbulent kinetic energy, being composed of the partial deviation in time and the advective change of turbulent kinetic energy by the mean flow

$$\frac{D}{Dt}k = \frac{\partial k}{\partial t} + U_i \frac{\partial k}{\partial x_i} \tag{5}$$

with U being the statistical mean flow velocity. In full notation the equation for the turbulent kinetic energy (after *Kundu* [1990]) is as follows

$$\frac{D}{Dt}k = -\frac{\partial}{\partial x_j}\left(\frac{1}{\rho_0}\langle p u_j\rangle + \frac{1}{2}\langle u_i^2 u_j\rangle - 2\nu\frac{\partial}{\partial_j}k\right) - \langle u_i u_j\rangle\frac{\partial U_i}{\partial x_j} - \frac{g}{\rho_0}\langle u_3\rho'\rangle - 2\nu\langle e_{ij}e_{ij}\rangle. \tag{6}$$

In (6) k is the turbulent kinetic energy per unit mass, u_i are fluctuations in velocity with the index denoting the direction in space (index 1 and 2 give the two horizontal directions, index 3 gives the vertical direction), ρ_0 is the mean density of water, ρ' is the fluctuation of water density and the overlining bars give statistical means. The first three terms on the right hand side of (6) represent the spatial transport of turbulent kinetic energy T from (4), with the first two terms representing the transport by turbulence itself and the third term being the viscous transport. The fourth term represents the shear production

$$P = -\langle u_i u_j\rangle\frac{\partial U_i}{\partial x_j}.$$

This term is usually positive and represents the loss of mean kinetic energy by the interaction of Reynolds stress with the mean shear. This term is a loss in the mean kinetic energy budget and a gain of turbulent kinetic energy. With boundary layer approximation, it is assumed, that all variables except the pressure are horizontally homogeneous and only have vertical gradients. The horizontal pressure gradient is one of the driving forces and therefore has to be retained (*Umlauf* [2001]). The shear production reduces with boundary layer approximation to

$$P = -\langle uw\rangle\frac{\partial U}{\partial z} - \langle vw\rangle\frac{\partial V}{\partial z}.$$

The fifth term represents the buoyant production of turbulence

$$B = -\frac{g}{\rho_0}\langle u_3\rho'\rangle.$$

The buoyant production can be a gain for turbulence. When the background density profile in the water column is unstable, the turbulent density flux $\langle u_3\rho'\rangle$ is downward

and the turbulent kinetic energy increases because of convective motions. When the water column is stably stratified, the turbulent density flux is directed upward, resulting in a loss in turbulent kinetic energy by increasing the potential energy of the watercolumn.
The last term on the right hand side of (6) is the viscous dissipation

$$\varepsilon = 2\nu\langle e_{ij}e_{ij}\rangle$$

where the e_{ij} are the fluctuating rates of strain

$$e_{ij} = \frac{1}{2}\left(\frac{\partial u_i}{\partial x_j} + \frac{\partial u_j}{\partial x_i}\right)$$

In considerations of mean kinetic energy and mean flow, dissipation is a negligible term, but in the turbulent kinetic energy equation the viscous dissipation is of the same order of magnitude as the production terms P and B. It is the loss by viscous friction within turbulent eddies and it represents the loss or conversion from kinetic energy to heat.

One can see in the equation of turbulent kinetic energy, representing a quantity of mixing, that the shear in currents determines the production of turbulence and a stable density profile acts against stratification. In order to describe stratification, several physical quantities and nondimensional numbers are considered in 2.4.1 up to 2.4.6.

2.4.1 Buoyancy frequency

In a stratified fluid, a frequency can be defined which characterises free oscillations in a stably stratified fluid. This frequency is called buoyancy frequency or Brunt-Väisälä frequency. When a fluid particle is displaced vertically, it undergoes vertical oscillations, driven by the interaction of gravitation and buoyancy for a water volume with density ρ_0. When the fluid is stratified in a stable manner, gravitation forces the volume downwards, when it is lifted up into surrounding water with lower density and buoyancy force the volume upwards, when it is moved downwards into surrounding water with higher density than ρ_0. The buoyancy frequency N is defined by

$$N^2 \equiv \frac{-g}{\rho_0}\frac{\partial \rho}{\partial z}. \tag{7}$$

In a non-stratified fluid, the buoyancy frequency is zero, because a water volume with density ρ_0 has its equilibrium position everywhere in the water column of homogeneous density ρ_0. With an increasing density gradient, the buoyancy frequency increases. The buoyancy frequency is imaginary for unstably stratified fluids and hence undefined. In stably stratified fluids, the maximal frequency ω of internal wave motions is N, so that internal waves in a certain depth have a wave period larger than the period which is equivalent to the buoyancy frequency, $T_b = 2\pi/N$.

The Brunt-Väisälä frequency is a quantity describing the density gradient of stably stratified fluids, and it has to be greater than zero for stably stratified situations.

2.4.2 Gradient Richardson number

The Gradient Richardson number is a number in stratified fluids that combines the density gradient with the shear in currents. It compares the buoyancy frequency with the shear frequency and is defined by

$$Ri_g(z) \equiv \frac{N^2}{\left(\frac{\partial u}{\partial z}\right)^2 + \left(\frac{\partial v}{\partial z}\right)^2} \tag{8}$$

with $\overrightarrow{u} = (u, v)$ being the horizontal flow velocity. The gradient Richardson number is a nondimensional number, indicating the stability of stratification in a fluid. The nominator of (8) increases with the density gradient in the fluid, and the denominator term increases squared with the shear in currents that produces turbulence. In a stability analysis it can be found that linear stability of a stratified flow is guaranteed if the gradient Richardson number is greater than 0.25 anywhere in the flow. It is necessary to have $Ri_g < 0.25$ in the flow to allow convective overturning, but the flow is not necessarily unstable, when fulfilling that criterion. But with $Ri_g < 0.25$ one has a useful guide for the prediction of instability of a stratified shear layer, shown in laboratory (*Scotti and Corcos* [1972]) and geophysical observations (*Eriksen* [1978]).

2.4.3 Flux Richardson number

Not as easy to measure as the gradient Richardson number from (8) is the flux Richardson number, comparing terms of the turbulent kinetic energy equation (6). The flux Richardson number Ri_f is defined as ratio of buoyant destruction to the shear production of turbulent kinetic energy. It is taking the fourth and the fifth term on the right hand side of (6):

$$Ri_f = -\frac{B}{P} = \frac{-\frac{g}{\rho_0}\langle w\rho' \rangle}{-\langle u_i u_j \rangle \frac{\partial U_i}{\partial x_j}} \tag{9}$$

For an unstable environment in which the density flux is downward, Ri_f is negative. The flux Richardson number becomes positive for a stably stratified environment. When having a large negative Ri_f, there is strong convection and weak mechanical turbulence. For a flux Richardson number being greater than 1, turbulence is removed by buoyancy at a rate larger than the rate of production of turbulence by current shear. Observations (*Panofsky and Dutton* [1984]) show that turbulence is decaying when there are turbulent fluctuations and a value of Ri_f larger than the critical value of about $Ri_{f\ crit} = 0.25$ is measured.

2.4.4 Turbulent Prandtl-number

The flux Richardson number and the gradient Richardson number as number stated above are related to each other by the turbulent Prandtl number Pr, being defined

as

$$Pr = \frac{Ri_g}{Ri_f} = \frac{\nu_t}{\nu_t'} \tag{10}$$

With the eddy coefficient assumption that parameterises the vertical Reynolds stresses as turbulent viscosity with the so called eddy viscosity ν_t and vertical turbulent density fluctuations as turbulent diffusion with the so called eddy diffusivity ν_t'. The eddy coefficient assumptions are

$$-\langle w\rho' \rangle = \nu_t' \frac{d\rho}{dz}$$

$$-\langle uw \rangle = \nu_t \frac{dU}{dz}$$

where ρ' is the fluctuation in density, w and u are the fluctuation in vertical and horizontal velocity and U is the mean flow velocity. The turbulent Prandtl number is greater than 1 for a stably stratified environment, because stratification damps the vertical transports of density and momentum, but the vertical transport of momentum is suppressed less, because possible internal waves can transfer momentum, but not density.

2.4.5 Froude number and Bulk Richardson number

A nondimensional number describing the flow in a fluid is the Froude number Fr. It relates the velocity in the flow to the velocity of shallow water waves

$$Fr = \frac{U}{\sqrt{gH}} \tag{11}$$

with g denoting the gravitational acceleration, U being the vertically averaged velocity and H being the water depth. When looking at a certain layer in a two-layered fluid, g has to be substituted by the buoyancy reduced gravity g', defined by

$$g' = g \cdot \frac{\Delta\rho}{\rho_0}$$

and the water depth has to be substituted by the layer height h, then the internal Froude number is calculated as

$$Fr_{layer} = \frac{U}{\sqrt{g'h}},$$

where U is near the average velocity in that layer The ratio in (11) is between 0 and 1 for a flow, in which waves can propagate upstream and downstream. A flow is called critical for $Fr = 1$, that means the waves cannot propagate upstream, but the crest of the wave remains at the place of disturbation. In supercritical flows with $Fr > 1$, waves propagate only downstream when the Froude number is big, gravitational effects can be neglected. The squared Froude number is the ratio of

inertial forces to gravitational forces in a fluid layer, inverting the squared Froude number gives the bulk Richardson number

$$Ri_b = \left(\frac{1}{Fr}\right)^2 = \frac{\frac{g}{\rho_0}\frac{\Delta\rho}{H}}{\frac{U^2}{H^2}} \tag{12}$$

2.4.6 Potential energy anomaly

A number that handles stratification in terms of energy including gravitation is the potential energy anomaly. A volume of heavy water at the seabed needs more energy to move upwards and mix with surface water than a volume of same size and density that resides closer to the surface. *Simpson and Bowers* [1981] define this anomaly of potential energy as

$$\phi = \frac{1}{H}\int_{-H}^{0} (\rho - \hat{\rho})\, gz dz \tag{13}$$

with the mean density

$$\hat{\rho} = \frac{1}{H}\int_{-H}^{0} \rho dz,$$

where z is the vertical coordinate (positive upwards), $\rho(z)$ is the density profile in a water column of depth H. This anomaly of potential energy is zero for a fully mixed water column. All stratified situations with differences in ρ give a change in ϕ, weighted with the water depth. The anomaly of potential energy becomes positive for a stable stratified water column and it becomes negative for an unstably stratified water column. Physically, ϕ gives the amount of energy per volume that is necessary to mix the whole water column up, bringing about complete vertical mixing. The unit of ϕ is $[J/m^3]$.

In several studies, ϕ has been used to quantify the stability of a water column, see e.g. *Simpson et al.* [1990], *Rippeth et al.* [2001], *Wiles et al.* [2006].

3 Setup for GETM Limfjord Model

For a foundation of the studies presented here, a basic GETM Limfjord simulation was set up[1]. This setup contained the model code with a compilation script and all the necessary input files like topography, reasonable input constants, simple initial conditions and boundaries. An important step and task for the present studies is to work on the basic GETM Limfjord simulation in order to develop a more realistic and exact reproduction of the Limfjord dynamics. In order to improve the model setup, the behaviour of the basic setup has been studied with the focus on how it works. Improvements have been introduced where the original setup behaved in an unrealistic manner.

3.1 GETM - the model code

GETM is an abbreviation for General Estuarine Transport Model. GETM is a fully baroclinic ocean-circulation model with hydrostatic and Boussinesq assumption (*Burchard and Bolding* [2002], *Burchard and Beckers* [2004]). The model has implemented a free surface with drying and flooding. The turbulence closure models are taken from GOTM (*Burchard* [2002], *Umlauf et al.* [2005], *GOTM* [2005]) and GETM works with the eddy viscosity assumption.

GOTM (General Ocean Turbulence Model) is a one-dimensional water column model for marine and limnological applications. It is coupled with a choice of traditional as well as state-of-the-art parameterisations for vertical turbulent mixing. Every discretised water column in the model is handled by GOTM to calculate turbulence quantities.

The numerical discretisation in the model is done with finite-volumes and finite-differences on an Arakawa C-Grid (see *Arakawa and Lamb* [1977]). On this grid with indices *i,j,k* constituting the X-points, temperature, salinity, pressure and sea surface elevation are given in the centre of the volume on the so called T-points. Horizontal velocities are given between the centres of volumes in the horizontal, called U-points and V-points. And the vertical velocities and turbulence quantities like eddy viscosity and eddy diffusivity are given between the volumes in the vertical, called W-points (see Figure 4). As transformations for discretisation in space, GETM can use orthogonal curvilinear coordinates, spherical coordinates, spherical orthogonal curvilinear or Cartesian coordinates in plain, and general vertical coordinates or sigma coordinates in the vertical.

GETM is implemented with mode splitting between barotropic and baroclinic mode. Mode splitting means to calculate the fast changing free surface and the resulting integrated velocities with a finer resolution in time than slow changing baroclinic variables like salinity and temperature, vertically resolved currents and turbulent quantities. These different timesteps are called micro timestep for the barotropic mode and macro timestep for the baroclinic mode. Bed friction is imple-

[1] thanks go to Karsten Bolding for preparing the model setup

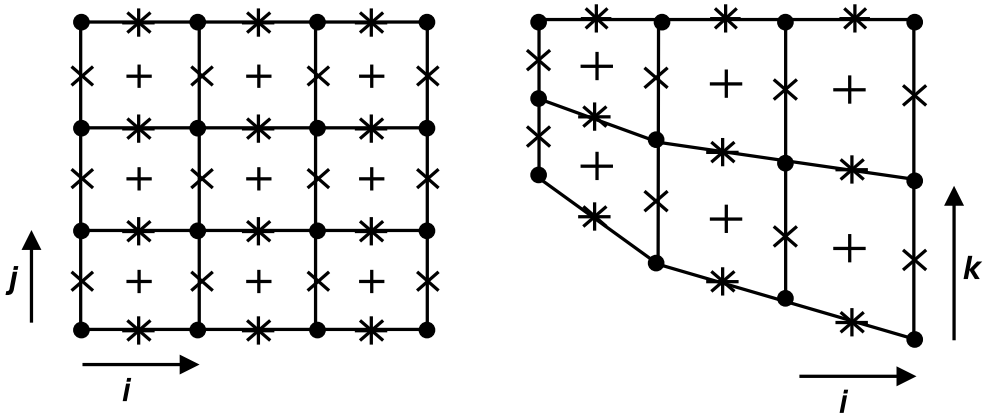

Figure 4: numerical discretisation (left: horizontal, right: vertical) on an Arakawa C-grid. •: X-points, +: T-points, ×: U-points, ∗: V-points in horizontal and W-points in vertical

mented by a logarithmic law assumption for the velocity in the near-bottom layer with the bottom roughness length as tunable parameter for friction stresses and logarithmic law itself (see 2.3.2). This bottom roughness length is constant for the whole model area.

The GETM code is written in Fortran 90/95 with a modular code structure and prepared for parallel computing. Input and output data can be handled as the binary, self-describing NetCDF format. GETM and GOTM are public domain models under GNU Public Licence.

3.2 Calculation environment

The GETM Limfjord Model runs on a 4-PC computation cluster of Bolding & Burchard Hydrodynamics, located at IOW. The hardware specification of each PC is Intel Pentium 4 2.8 GHz; 1024 MB RAM; 150 GB harddisk. All PC's were connected via 100 Mbps Ethernet Network. The PC's were running with the Linux operating system Debian Sarge with Kernel 2.6.8. The installed and used software is: NetCDF v3; MPICH v1.1.2; NCO-tools v2.9.9; GETM 1.3.2; GOTM 3.1.3; gcc v3.3.6; Intel Fortran Compiler v8.0;

One of these PC's is the master computer hosting the /home directory. This directory is nfs-mounted on every other PC, so that that the model (GETM,GOTM) and the setup, containing the input files, are stored consistently. Each PC has its own /data directory at the local disk for storing the output files without using the network. The model starts running by calling MPICH on the master computer for running the compiled model executable. The input you have to give to MPICH is a machine file and the number of calculation jobs. This number and the number of machines in the machine file have not to be identical, it is possible to send more than one job to one machine. The GETM Limfjord Model consists of 16 calculation

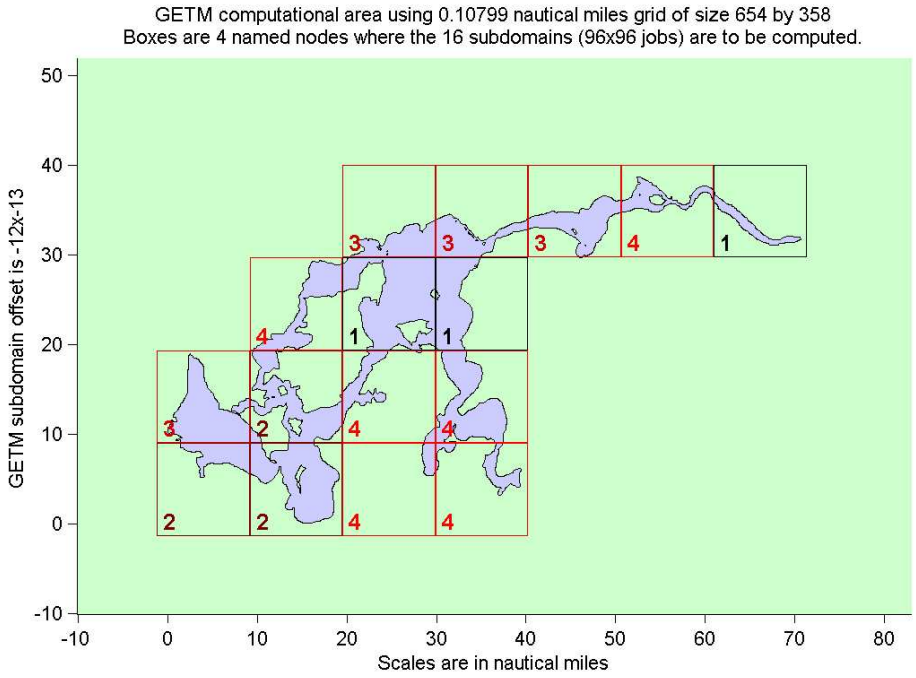

Figure 5: Computation Map for the GETM Limfjord Model on the BBH cluster at IOW (Warnemünde)

domains, that means 16 calculation jobs, running on 4 machines. The machine file gives a list of network names of computers the model should run on. MPICH reads in the configuration file for parallel computing (machinefile) and starts running the single domains on the nodes like mentioned in the machine file. The master computer has to run the first domain. On the nodes, the running executable is reading in the input files of the setup. These input files are located in the nfs-mounted /home-directory. The output is stored on the local /data partition directly on the node. After every timestep, all domains have to exchange their neighbour data. The information about which points have to be exchanged and who's the neighbour is given in the file par_setup.dat and was put into the model's executable during compilation.

The GETM Limfjord Model was splitted into 16 domains with 96x96 points in each of them. These 16 domains are distributed on the cluster of 4 machines like in Figure 5. This map and the corresponding machinefile are produced by a matlab script (*Buechmann* [2004]). By running this script, matlab reads out the number of water points in each domain and distributes the domains to the four machines in the cluster, so that each machine has to calculate for approximately the same number

of water points. The whole computation time is proportional to the time needed by the machine with the maximum number of water points, because all machines have the same processor and have to wait for the slowest after every timestep.

3.3 Grid and Coordinates

The GETM Limfjord Model was set up with a Cartesian horizontal grid with a resolution of 200m in the east-west direction and 200m in the north-south direction. The area of the Limfjord measures about 130x70 km and therefore a spherical grid is not necessary. The meridional length of less than one degree in latitude will allow one handle this area as f-plane where the Coriolis frequency will be set as constant and not depending on the location within the grid. In the GETM Limfjord Model, the Coriolis frequency was calculated from latitude 57.0°.

The vertical setup for the GETM Limfjord Model was realised in general vertical coordinates with a discretisation of 10 vertical layers. This discretisation in general vertical coordinates introduces internal surfaces z_k with $k = 0, .., 10$, which do not intersect, each depending on the horizontal position (x, y) and the time t. In the Limfjord Model, z_0 is the sea bed and z_{10} is the sea surface. As distribution of these internal surfaces, GETM uses horizontally varying σ-coordinates (first applications by *Freeman et al.* [1972] for natural waters and *Phillips* [1957] for the atmosphere)

$$\sigma_k = \frac{k}{N} - 1 \tag{14}$$

with $N = 10$ and $k = 1, .., N$ in this case and

$$z_k = D\sigma_k$$

This σ-coordinates can be refined towards the surface and the bed. This refinement is controlled by the parameters d_l for lower zooming and d_u for upper zooming

$$\beta_k = \frac{\tanh((d_l + d_u)(1 + \sigma_k) - d_l)) + \tanh(d_l)}{\tanh(d_l) + \tanh(d_u)} - 1 \tag{15}$$

with z-levels obtained as follows

$$z_k = D\beta_k,$$

see *Burchard and Bolding* [2002]. General vertical coordinates are an interpolation of these two coordinate distributions in order to have an equidistant grid in shallow areas for a good resolution of stratification near the surface as well as near the bed and the advantage of a higher resolution at the surface and near the bed with a refinement like the β distribution in (15). D_γ is the critical depth where the coordinate distribution changes from σ-coordinates in shallower regions to β-coordinates in deeper regions. The internal surfaces are defined by

$$z_k = D(\alpha_\gamma \sigma_k + (1 - \alpha_\gamma)\beta_k)$$

with σ_k from (14), β_k from (15) and

$$\alpha_\gamma = \min\left(\frac{(\beta_k - \beta_{k-1}) - \frac{D_\gamma}{D}(\sigma_k - \sigma_{k-1})}{(\beta_k - \beta_{k-1}) - (\sigma_k - \sigma_{k-1})}, 1\right)$$

In the GETM Limfjord Model, the parameters are used as follows:

d_u	$= 2.0$
d_l	$= 1.0$
D_γ	$= 10.0$ m

This means that the model uses σ-coordinates for areas with a depth below 10 meters and a zoomed σ-coordinates with a finer grid at the surface than the refinement at the bottom. Figure 6 shows a picture of the layer distribution in Løgstør Bredning and the channel Hvalpsund.

The Navier-Stokes-equations derived for this type of vertical grid are described by *Burchard and Petersen* [1997]. They first transform the equations into general vertical coordinates and then integrate these transformed equations over constant intervals in the transformed space.

3.4 Boundary Conditions and initial conditions

As boundary conditions, GETM uses elevations, salinity and temperature at the open boundary points. In the GETM Limfjord Model, there are two open boundaries, one at the North Sea side and one at the Kattegat side. Each boundary consists of one gridpoint, because these boundaries are thin channels. As boundary values, hourly observed data for elevation from Nordjyllands Amt are used. Temperature and salinity data are being observed by Nordjyllands Amt every three hours. They are linearly interpolated in time where no observational data was accessible.

Sea surface elevations, out of the 2D boundary input file, are linearly interpolated in time, so that there exists a boundary elevation at every micro timestep for the open boundary points. The maximum of the two values, boundary and a critical depth, being the residual water depth of dry water points, is entered directly into the model as sea surface elevation ζ.

As boundary conditions for velocities at open boundaries, GETM prescribes the gradient of velocity across the boundary, normally to the horizontal gradient ($\vec{\nabla}_h = (\partial_x, \partial_y)$) of the open boundary, to be zero.

The boundary values, out of the 3D boundary input file, for temperature and salinity, given from measurements (like with the GETM Limfjord Model) or results from other simulations, are linearly interpolated in time to have a boundary value every macro timestep. Vertically, these boundary values are interpolated linearly onto the layer grid. Because of the fact that the boundaries in the GETM Limfjord Model are shallow and narrow channels to North Sea and Kattegat it was assumed,

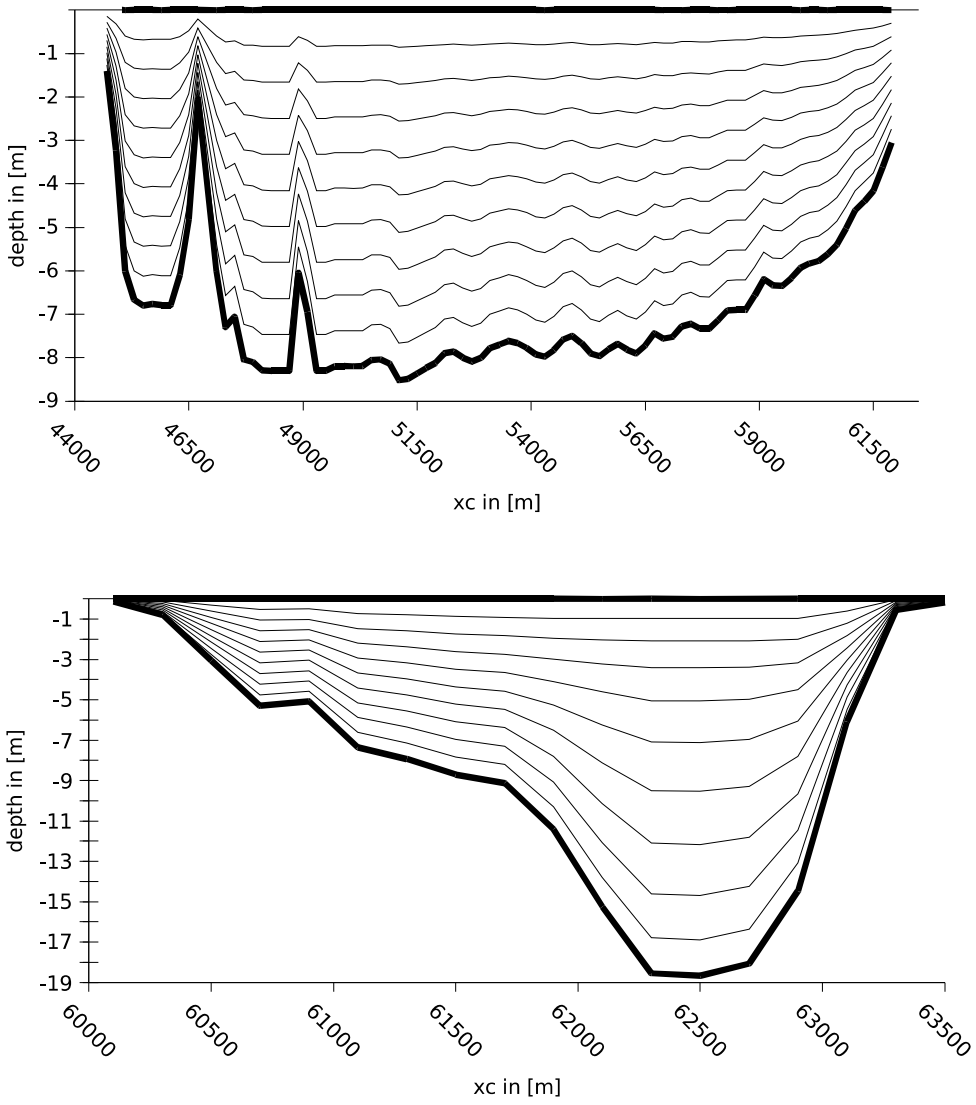

Figure 6: Vertical slices (above: slice through Løgstør Bredning northerly of Livø, below: slice through Hvalpsund) with layer surfaces.

that turbulence generates a mixed water column. Therefore, temperature and salinity are vertically prescribed in the boundary conditions as only one value each. This value was interpolated as a constant value over depth.

The baroclinic variables temperature and salinity are implemented with a sponge layer according to *Martinsen and Engedal* [1987]. This sponge layer is an area, including the boundary and reaching three neighbouring water points from the boundary into the model. Temperature and salinity in this area have an abating influence on the boundary values, depending on the distance from the boundary. A property A at the eastern boundary with a boundary value A_{bdy} is calculated as given in (16). In (16), i, j are horizontal indices with i being the index in direction of the sponge layer. The boundary point is at index $i = 1$, the sponge layer reaches from $i = 1, .., 4$. The property A is at this timestep not affected by the boundary from index $i = 5$ above.

$$A_{new}(i,j) = A_{bdy} \cdot sp(i) + A_{old}(i,j) \cdot (1 - sp(i)), \qquad i = 1, .., 4 \tag{16}$$

with sponge values $sp(i)$ as follows

$$\begin{aligned} \mathrm{sp}(1) &= 1.0 \\ \mathrm{sp}(2) &= 0.5625 \\ \mathrm{sp}(2) &= 0.25 \\ \mathrm{sp}(4) &= 0.0625 \ . \end{aligned}$$

For initial conditions, it is impossible to have a realistic 3D field of temperature and salinity out of observations for the whole area. An oceanographic model including the Limfjord would be the only way to obtain a 3D field, but such data was not accessible. An initial condition can also be created out of several measurements, being extra- and interpolated. By starting modelling with realistic forcing and boundaries, it can be assumed that the model "forgets" its initial conditions. With a model period of the year 2003, starting at 1 January, a rough initial condition for temperature was used: The temperature was set to 3 °C for the whole 3D-field. Because changes in temperature are fast in these shallow waters and these changes are local by heat flux and radiation, temperature adjusts quickly. The salinity initial condition was set more precisely: The Limfjord was vertically set to non-stratified, but has spatial differences. One can see in the observations of monitoring stations in the Limfjord that salinity is quite high and not stratified in Thisted Bredning (31 PSU at 1 January, 2003), thus decreasing eastwards. In most parts of the Limfjord, salinity is around 20-23 PSU. In Løgstør Bredning, salinity is around 22 PSU. To keep the initial conditions simple, salinity was set to 22 PSU in the eastern part of the Limfjord, but increases westward of Løgstør Bredning linearly to 31 PSU. For an overview, see Figure 8. The initial elevation is zero for the whole Limfjord.

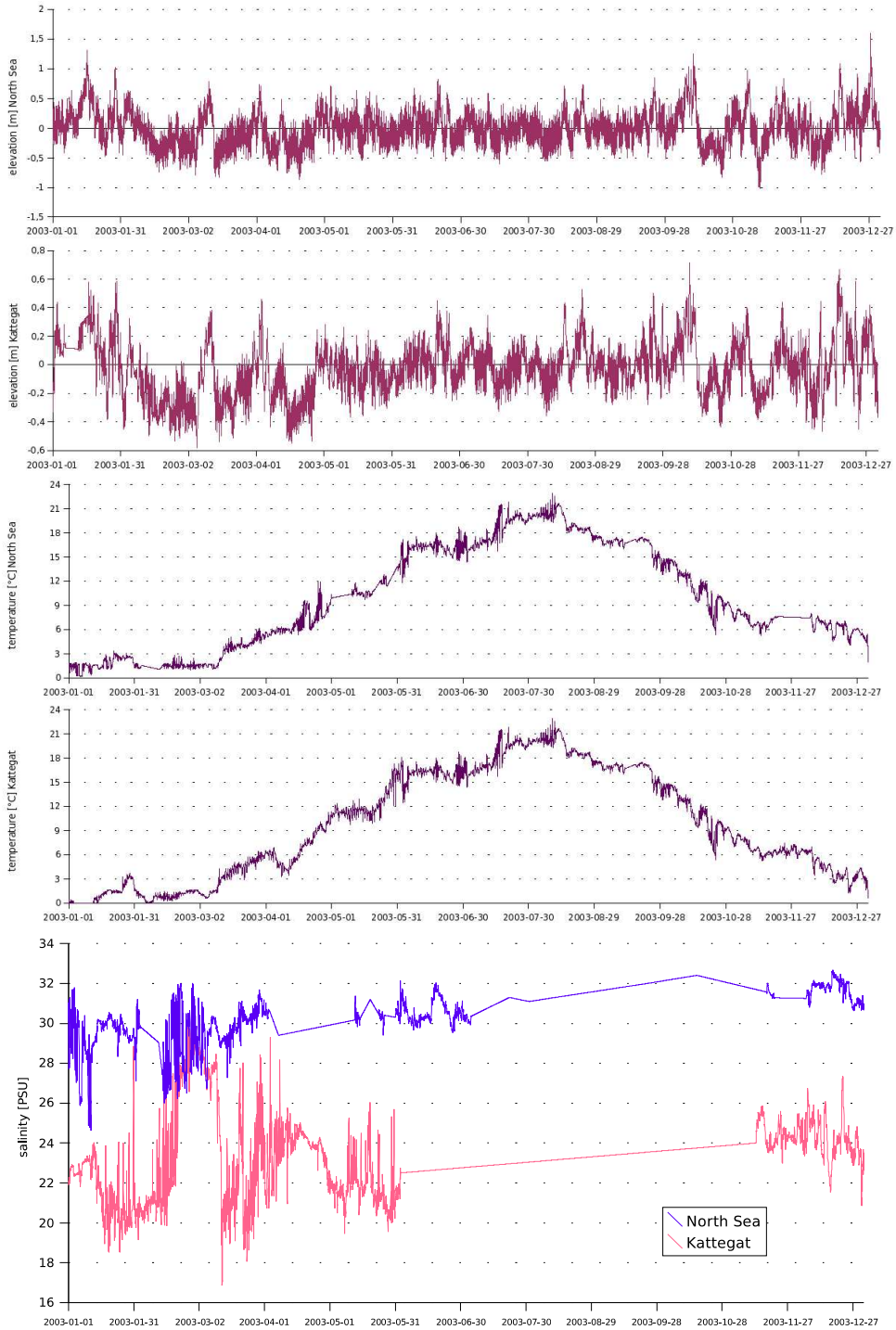

Figure 7: Boundary data for GETM Limfjord Model. Above: sea surface elevation, middle: temperature, bottom: salinity

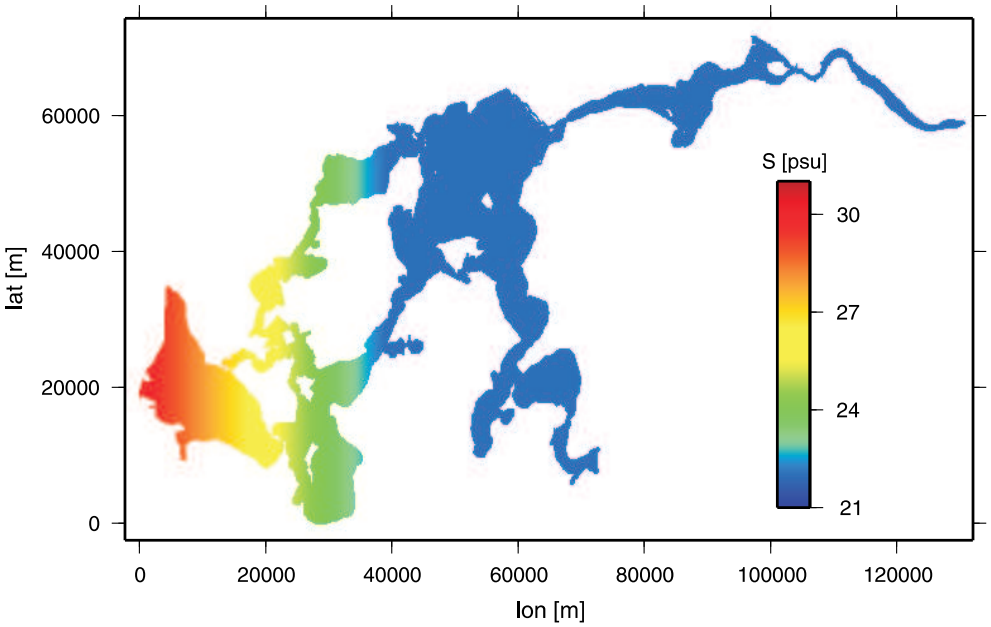

Figure 8: Initial salinity for GETM Limfjord Model on 1 January, 2003

3.5 Meteorological Forcing

As meteorological forcing, model data from the German Weather Service Local Model (DWD-LM) were used. These data contain air temperature, dew point temperature, humidity and air pressure in 2m above sea surface, and eastward and northward wind velocity in 10m above sea surface. The time interval of these data is 3 hours. This meteorological forcing is given at only one point in the model, because it is a local model with a horizontal range of 130x70 km. It can be assumed that the meteorological forcing does not change a lot within this area. To validate this forcing data from a weather model against measurements, one can use the observed weather data during the Limfjord campaign in 2003. The values were taken from the Isle of Livø every 10 minutes. To compare this data, air temperature and wind speed are compared between model and observations, see Figure 9.

One can see that the DWD-LM model comes close to the observed results and contains all observed events. There are differences of 1.51 °C rms in temperature and 1.46 m/s in wind speed. These differences may be caused by the fact that the model point is on water and the observation point is on land. The temperature may be less than the observed values, because in the DWD model the heat is used for evaporation of unrealistically assumed water on land in spring 2003.

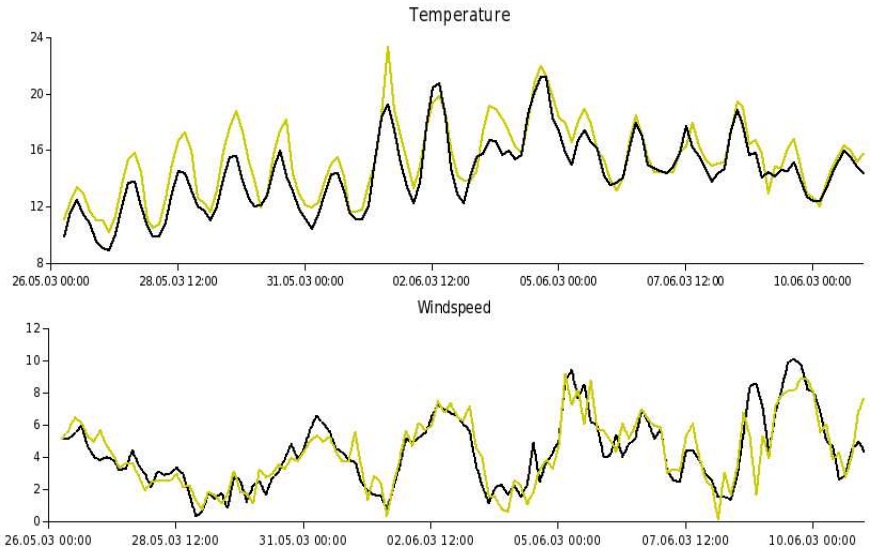

Figure 9: Meteoforcing Comparison Model-Observations; temperature above, windspeed below

3.6 Improvement of the model setup

The first model run was carried out until June 2003. That simulation took about 5 days and the results were stored every hour for barotropic 2d variables and every 6 hours for the whole 3D field (salinity, temperature, density, velocities, dissipation, turbulent kinetic energy). These data of 6 months took 60GB on the harddisk. The initial conditions were a bit different than given above. The model starts running with a linear salinity gradient in the east-west direction for the whole area from 32 PSU at the North Sea side to 22 PSU at the Kattegat side. The initial salinity was homogeneous in depth. First comparisons with salinity observations showed a too high salinity in the end of May, starting already in January with 26 PSU in Løgstør Bredning and increased up to 29 PSU in the end of May. Observations showed that there should be a salinity of around 23 PSU. Another problem was the temperature at the end of May. It was around 6 °C at a depth of 8m, but should have been around 12 °C. These two parameters are very important when one wants to look at stratification. When there is an unnatural inflow of saline water, there should be an overestimated stratification. If the solar radiation does not warm the water enough, there should be an underestimated stratification, because no lighter water at the surface is produced. There were two major problems:

1. too high salinity in the Limfjord,

2. too low warming by solar radiation.

In order to solve the salinity problem, there are many different methods to choose between. One major point is the lack of freshwater inflow by rivers, ground water

and precipitation. Precipitation is not a major point against river inflow and it was not implemented into the model at the time being, so precipitation is not considered. Another point will be the initial salinity. When there is salinity in the Limfjord with its narrow channels, it will take a lot of time to mix this additional salinity up by freshwater inflow. In reality, this freshwater inflow mixes up the saline inflows from the North Sea - when we set up observed freshwater inflow, it will not be able to mix up the saline inflows from the North Sea and the additional salinity from the initial conditions. These conditions have to be changed in a way, so that there is a more or less realistic salinity in the beginning of 2003. A next point to better salinity is to get maybe more realistic, smaller inflows from the North Sea side. When realistic river inflows fall short of the real results, the saline inflows must be either too strong, or the less saline inflows from Kattegat must be too weak. This could be a question of centimetres in the elevation measurements or an error or an effect of a bad bathymetry or the coarse resolution of bathymetry. A comparison with sea charts does not give an indication for a bad bathymetry, except in one channel that was too wide in the bathymetry.

3.6.1 Improvement of Bathymetry

When looking at a sea chart of the Limfjord (*BSH* [1997]), almost the mapped bathymetry looks like being well represented by the 200mx200m bathymetry-file. There may be certain points where errors have occurred in the digitalising process, especially the island Ejerslev Røn and some surrounding points and the coastal area southern of Thyholm had to be corrected simply by taking values near to the sea chart (*BSH* [1997]).

But these small areas beside the main flow will not have a significant effect. The channel between Sunddraget and Grisetåodde was too wide on the original bathymetry file compared to the sea chart (*BSH* [1997]). Narrowing this channel by one third (see Figure 11) had a significant effect on the throughflow through this channel. Its depth is quite well represented by the bathymetry file.

A study about the adjustment of the bathymetry was carried out by changing the bathymetry in certain areas and calculating the transport at a narrow channel east of Løgstør Bredning. There, the model has only four grid boxes and the channel is directed eastwards, so a simple calculation to estimate the mean transport was used.

$$Transport = \sum_{4\ boxes} H_{box} \times 200m \times u_{box} \tag{17}$$

These studies contain five cases with different changes in the bathymetry. The first two changes were a percental change of the whole bathymetry by 5% and 10%. These changes should decrease the transport by having more friction in the whole watercolumn. The third change is an artificial change. A box was put into the Salling Sund at the coast in order to narrow the channel, but only in the shallow parts of Salling Sund. The maximal depth was not changed. Cases 4 and 5 are

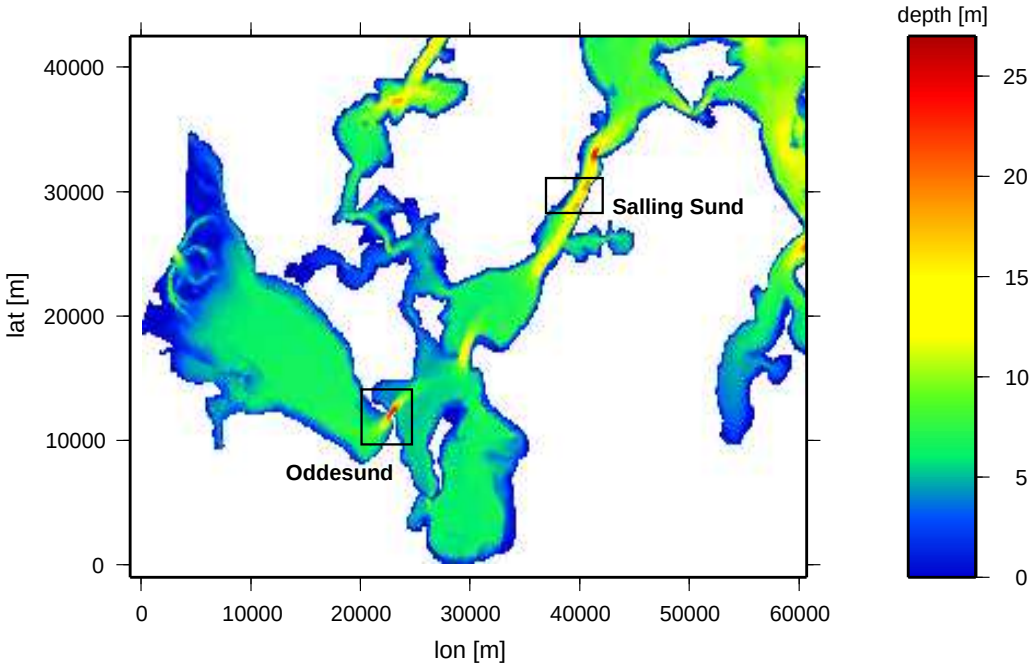

Figure 10: Southwestern part of the Limfjord with Oddesund and Salling Sund being marked

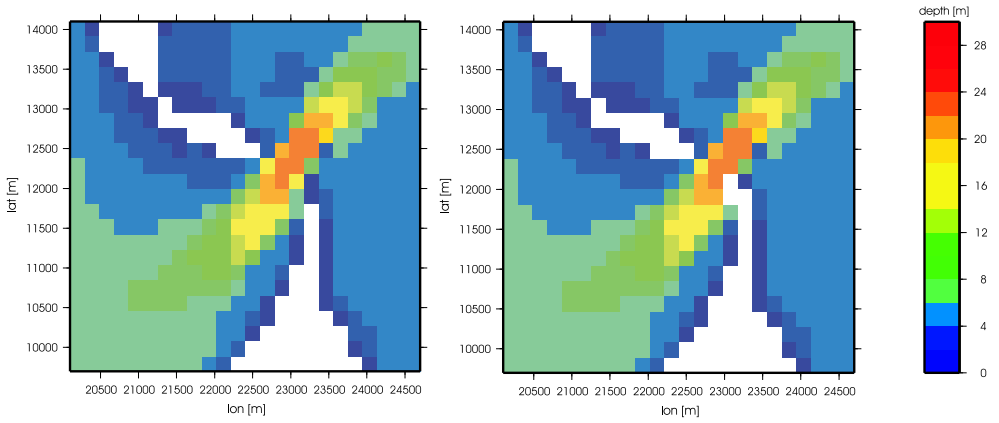

Figure 11: Changes at Oddesund, the old bathymetry is on the left hand side, the new bathymetry is on the right hand side

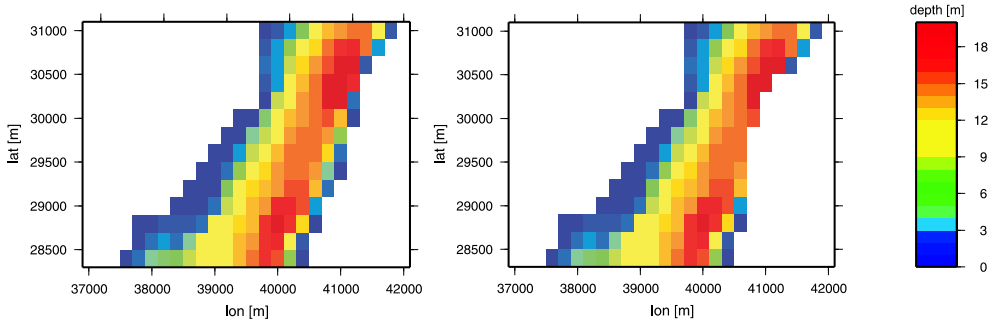

Figure 12: Changes in Salling Sund within case 4 of transport studies, left: original bathymetry, right: boxes in Salling Sund

related to changes of elevation at the North Sea side and the Kattegat side. Two setups were studied: In Case 4, the mean difference in these elevations is half of the observed difference (5cm below observed difference in elevation) and in Case 5, the mean difference in these elevations is set to zero, so mainly the wind and short lasting differences in elevations at North Sea and Kattegat drive the saline inflows. The results for the transport after Eq. (17) calculated with hourly values for u_{box} are given in Table 1.

Case	Transport in m^3/s	relative Transport
original bathymetry	23.68	1.0
bathymetry minus 5%	22.15	0.94
bathymetry minus 10%	20.67	0.87
box in Salling Sund	23.67	0.9997
SSE North Sea minus 5cm	19.31	0.82
SSE North Sea minus 10cm	14.79	0.62

Table 1: Transports carried out by transport studies with several changes in the bathymetry of the GETM Limfjord Model

One can see in these studies of the throughflow through the Limfjord, that the inflow of saline water from the North Sea, is most sensitive to changes in the difference of sea surface elevation between the North Sea and Kattegat boundary. Changes for the whole bathymetry will render the bathymetry of the model unrealistic, because the original bathymetry is almost like the bathymetry on the sea chart. Changes, like strongly narrowing wider channels such as Salling Sund, do not have a significant effect. These changes may be due to a bad coastline and will be in the magnitude of only one gridbox.

The adjustment of the bathymetry was undertaken only in special points where

the digitalisation failed and in narrowing of the channel at Sunddraget. In order to adjust the inflow from the North Sea, the transport studies show that it is advisable to decrease the difference of the sea surface elevation between the North Sea and the Kattegat boundary.

3.6.2 Freshwater inflow

In the model, freshwater inflow will take place via the inflow of the rivers. In reality this freshwater inflow will be precipitation, groundwater and rivers. The rivers flowing into the Limfjord are not that large, but the more diffuse freshwater inflow by little rivers along the Limfjords coast results in a freshwater volume of 2.4 km^3/year. This diffuse freshwater inflow as well as the precipitation on the land, which does not evaporate but flows into the Limfjord via small rivers, will be included in the runoff data.

GETM registers freshwater inflow from all the rivers by means of a specially set up river specification file (riverinfo.dat), that specifies the assignment of rivers in the model grid. A river may consist of more than one point, then each point is handled like a river with runoff-value divided by the number of points, the river consists of. In a special netcdf file are the runoff values for each river and timestep. GETM handles runoff values in m^3/s. The runoff values for each river and timestep are stored in a special datafile of the rivers (rivers.nc netcdf file was used in this case). The unit of this values has to be in Volume per time. In the GETM inputfile (getm.inp) a factor has to be set, which will be multiplied with the values in the rivers datafile. The outcoming product has to be a runoff value in m^3/s. It is possible to have data in km^3/day in this file and set the factor to 8.64×10^{-5}, for example. The inflowing volume is calculated by

$$V_{river} = t_{timestep} \times v_{runoff} \times \frac{1}{N_{this\ river}}. \tag{18}$$

This volume is added to the volume in the watercolumn by increasing the sea surface elevation. Every micro timestep, the model increases the elevation by the height of water volume (index μ stands for micro, index m stands for macro):

$$height = V_{river} \cdot \frac{1}{A_{gridbox}},$$

$$\eta_\mu = \eta_\mu + height.$$

In the 3D mode, GETM cumulates these micro timestep heights to get the additional height per macro timestep , but adds this macro_height to the sea surface elevation after handling layer heights and salinities (in baroclinic mode) for every layer:

$$macro\_height = \sum_{i=1}^{N_{\mu/m}} height_i,$$

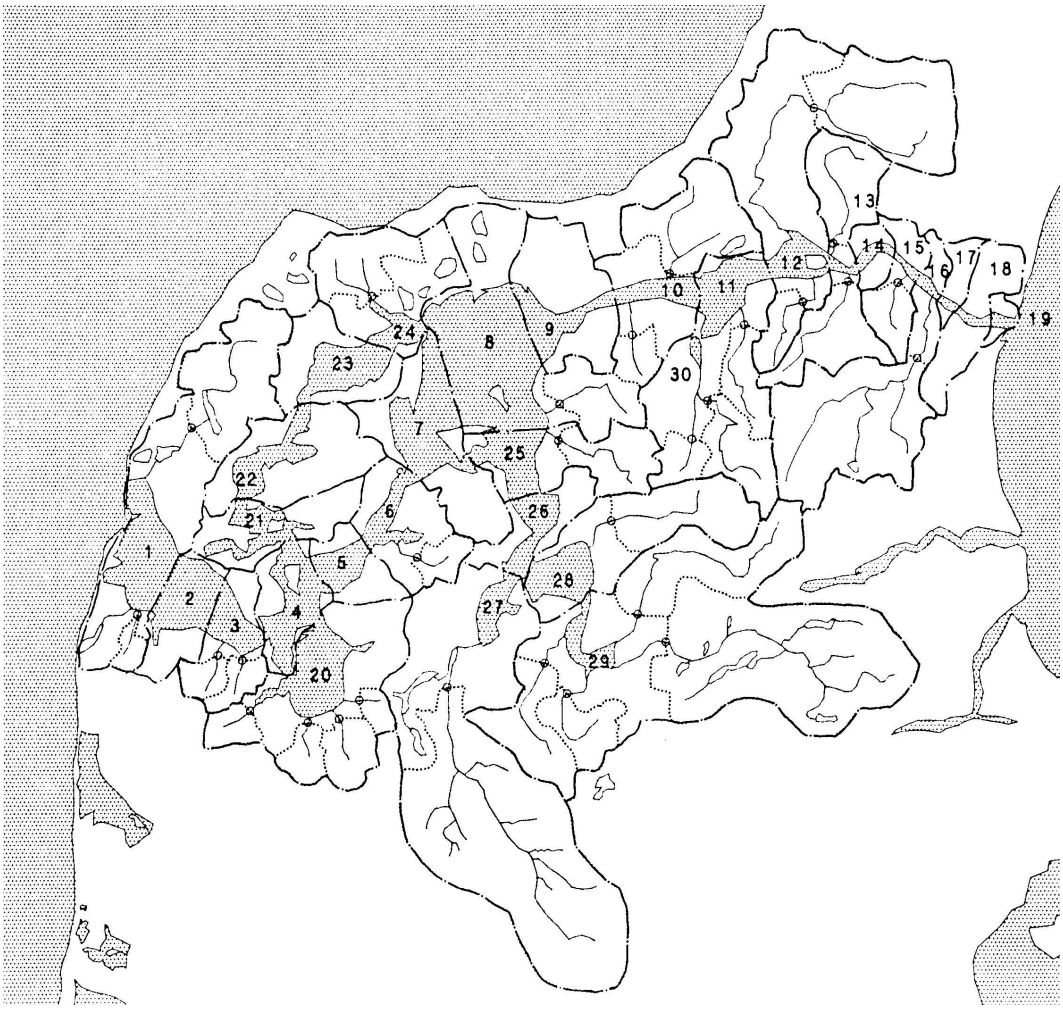

Figure 13: Catchment area map used for freshwater input into GETM Limfjord Model

$$S(layer) = S(layer) \cdot \frac{\eta_m + H}{\eta_m + H + macro\_height},$$
$$h(layer) = h(layer) \cdot \frac{\eta_m + H}{\eta_m + H + macro\_height},$$
$$\eta_m = \eta_m + macro\_height.$$

In the GETM Limfjord Model, freshwater runoff data from Nordjyllands Amt have been used. These are observed monthly runoff data for 30 catchments areas, covering the coast of the Limfjord (see Figure 13). A cumulated value for 2003 for each catchment area is given in Table 2. Obviously, the most inflow occurs in

catchment areas 29 and 27. This will result in a low salinity in these areas, but also a strong stratification in direction of Løgstør Bredning, where the saline inflows from the North Sea will be confronted with the freshwater from the inflow of the rivers.

Simulations with this freshwater input showed a much lower salinity than without this freshwater input (the decrease is about 21% in Løgstør Bredning). This can be traced back to the fact that the input of freshwater of 2.4 km^3/year is about a quarter of the net west-east flow-rate of 8.7 km^3/year. The freshwater input was the most important tool to get a realistically modelled salinity.

3.6.3 Adjusting the sea surface elevations

The transport studies in 3.6.1 show that the transport through the channel to Kattegat is very sensitive to changes of sea surface elevations at the boundaries. The difference of sea surface elevations between the North Sea boundary and the Kattegat boundary drives a mean throughflow and inflow volume from the North Sea. When there are problems caused by the discretisation in bathymetry or problems by the constant bottom roughness, this could be compensated by a slightly changed sea surface elevation at the boundaries. With a constant realistic river inflow it is even possible to control the modelled salinity in the Limfjord by setting the realistic throughflow by tuning boundary sea surface elevations. The aim of adjusting the sea surface elevations was a realistically modelled physical behaviour in the Limfjord, which is why salinity became an indicator for a realistic combination of the river inflow and the wets-east flow of the Limfjord. The monitoring station in Løgstør Bredning was taken as reference for salinity and sea surface elevations were adjusted in the first six months of 2003 so that there would be minimal differences in salinity between measurements and the model. With a difference in boundary sea surface elevations between the west and the east boundary of 2cm, the modelled salinity was most realistic, compared to measurements in Løgstør Bredning.

3.6.4 Turbidity and residual radiation

When studying the heating of the water, the most sensitive way is to look at solar radiation and its influence on the water column. The first reduction of solar radiation occurs due to the reflection on the surface. This property is prescribed by the albedo value. It depends on the angle of radiation from the sun (depending on date, time and location on the earth) and denotes the amount of reflected light with a relative value between 0 and 1, where 0 means no reflection, the whole radiation enters the water column, and 1 means that the whole amount of radiation is reflected on the surface. The radiation that enters the water column is absorbed by particles and molecules in the water column. This absorption depends on the wavelength of the incoming radiation and the degree of absorption, depending on the composition of the water including the particles in it. The absorption obeys the exponential law

for the intensity of radiation depending on the distance from the surface d.

$$I(d) = I_0 \cdot e^{-\frac{d}{g}}$$

with g as e-folding length, depending on the wavelength. Absorption can be seen optically as turbidity of the water. In GETM, turbidity or absorption is implemented with a double exponential absorption function. The absorption properties are regarded as the absorption of two types of radiation, long wave radiation and short wave radiation. After *Paulson and Simpson* [1977], the double exponential absorption function with e-folding absorption lengths for each range of wavelength g_1 and g_2 is implemented as

$$R_k = R_0 \cdot \left(A e^{-\frac{z_k}{g_1}} + (1-A) e^{-\frac{z_k}{g_2}} \right), \qquad k = 0, .., N \tag{19}$$

with k being the layer index ranging from 0, for below the bottom layer, 1 for the bottom layer up to N, the number of layers, for the surface layer, A gives the amount of short wave intensity in the radiation flux through the surface, z_k is the depth and R_0 is the radiation flux at the surface, given in energy per time. The change in temperature per layer is caused by a difference between incoming and outgoing radiation in the layer

$$\Delta T_k = \Delta t \cdot \frac{R_k - R_{k-1}}{\rho_0 \cdot c_p} \tag{20}$$

with ρ_0 being the mean density of the water and c_p being the specific heat under constant pressure.

In the first simulation, temperatures were so low because of the wrong absorption coefficients which had to be changed directly in the model code. The water class of the Limfjord is approximated as Jerlov water class number 6 (*Jerlov* [1968])

A = 0.78, g1 = 1.40, g2 = 7.90

In the shallow areas there was a mistake in calculating ΔT by (19) and (20), because a significant rest of radiation is lost when the radiation reaches the bottom. Two processes were missing: one process including the reflection at the bottom and the heating of the bottom by radiation, the other process including the following heatflux into the water at the seabed by the heated bottom. As an approximation for those processes that have their effect mostly in the near seabed waters, the whole radiation that leaves the layer before the bottom layer is taken for heating the bottom layer as follows:

$$\Delta T_1 = \Delta t \cdot \frac{R_1}{\rho_0 \cdot c_p}$$

Catchment Area	Runoff in km^3/year	relative Runoff in %
29	0.394	16.1
27	0.322	13.1
12	0.213	8.7
1	0.137	5.6
16	0.116	4.7
24	0.114	4.7
8	0.103	4.2
28	0.101	4.1
10	0.097	3.9
20	0.095	3.9
30	0.09	3.7
13	0.087	3.5
22	0.071	2.9
7	0.07	2.9
25	0.065	2.7
21	0.055	2.3
6	0.046	1.9
11	0.046	1.9
9	0.038	1.6
3	0.03	1.2
23	0.03	1.2
26	0.026	1.1
5	0.025	1.0
4	0.021	0.9
2	0.016	0.7
14	0.016	0.6
15	0.01	0.4
17	0.01	0.4
18	0.004	0.2
19	0.002	0.1
whole area	2.451	100

Table 2: Runoff values for 2003 for catchment areas in Figure 13. Data from Nordjyllands Amt.

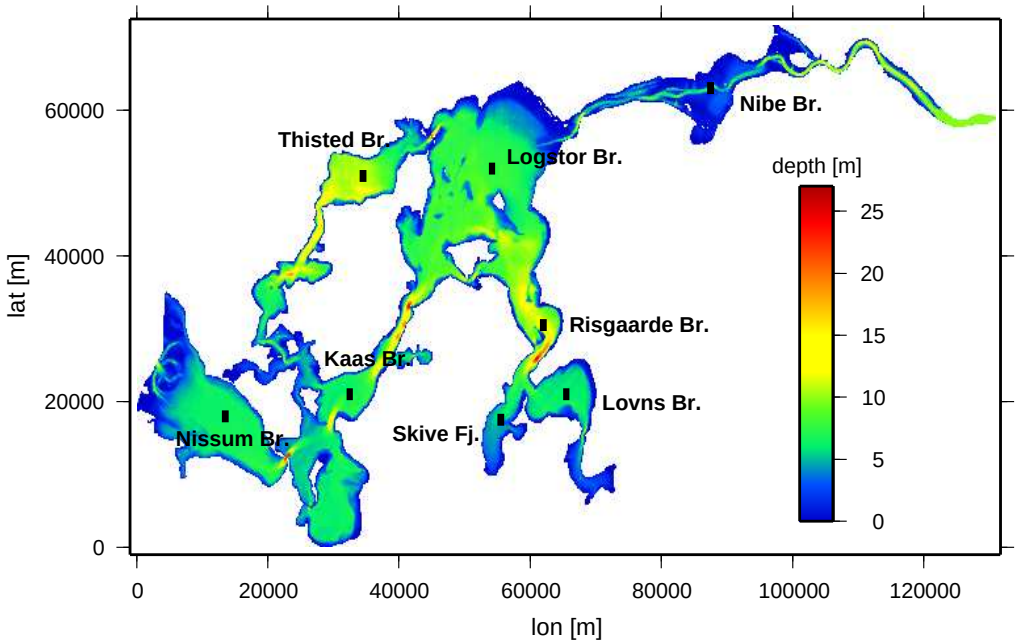

Figure 14: Points of monitoring observations in the Limfjord

4 Model results

4.1 Validation of the model results

In order to validate the model results, monitoring observations in Løgstør Bredning, Nissum Bredning, Kås Bredning, Thisted Bredning, Risgårde Bredning, Lovns Bredning, Skive Fjord and Nibe Bredning are used. In order to obtain a realistic value for stratification, the 4D field of density has to be modelled realistically. After the equation of state for potential density $\rho = \rho(S, \theta, p)$, one has to have realistic model results in the Limfjord for salinity and potential temperature. Because of the strong salinity gradient of 10 PSU between the North Sea and the Kattegat and the salinity gradient of 20 PSU in areas with river inflow, stratification, related to differences in the density ρ, will be correlated to differences in salinity. Temperatures play not such a big role, because the Limfjord is shallow and therefore the warming by solar radiation has an effect on great parts of the water volume in the Limfjord. The difference in temperature for a water column between sea surface and seabed are less than the differences in salinity. In general, temperature differences between sea surface and sea bed reach at maximum 6 °C for short times.

The different monitoring stations in the Limfjord are shown in Figure 14. As

a strategy for the comparison in this section, curves of bottom and surface values from the model and the observations are shown for salinity and temperature at every monitoring station in the following sections.

4.1.1 Elevations

As validation for elevations, observed data for Løgstør Bredning were compared to the model results. For the model data, the monitoring point for salinity and temperature in Løgstør Bredning was taken from the model and is compared with hourly values from sea surface elevation measurements (see Figure 15). The rms-difference between model results and observational data being centred measures 0.054 m. The elevations out of the GETM Limfjord Model behave very closely to the observations, and it can be seen that almost every event in the observed sea surface elevations can be reproduced by the model, even in quantity. A qualitative difference in the elevations can be seen at the beginning of the year 2003 - when the model was started. The first value in observations 1 January, 2003, at 00:00 clock is -5.7 cm. The model starts with zero elevation and starts running with an artificial initial salinity that produces artificial currents. But within the first 15 days of simulation, the model "forgot" the initial conditions in sea surface elevations. In general, the modelled sea surface elevation is a few centimetres below the observed sea surface elevation. Figure 16 shows a scatter plot of centred time series of modelled and observed sea surface elevations. The line in that figure gives the equality of both time series and the most points of the scatter plot are near the equality-line, the standard deviation between both time series is 10.6 cm. The mean difference in modelled and observed sea surface elevations measures 6.5 cm and is resulting from the throughflow adjustments (see 3.6.3). This difference may be a problem of different reference gauges as well as in 3.6.3.

4.1.2 Salinity

The figures 18 to 25 show graphs of bottom and surface salinity and bottom and surface temperature. These graphs contain monitoring observations (printed as squares) and model results (printed as lines). In general, the monitoring intervals for salinity and temperature are too large to validate the results in quantities. The mean monitoring interval equals two weeks and the model wrote out results every 6 hours (macro timestep). In all figures of salinity, it can be seen that the modelled salinity has the same magnitude than the observed salinity. The major events are represented by the model in nearly all monitoring points. In order to obtain a valid stratification information for the mussel producing area, the GETM Limfjord Model is adjusted in order to give valid results in Løgstør Bredning. In addition to Figure 18, Figure 17 shows a vertically resolved salinity over depth for the whole year 2003 at the monitoring station in Løgstør Bredning. The modelled salinity comes very close to the measured salinity, especially in the first six month of 2003. Since August 2003, one can see in Løgstør Bredning that the model is 1 PSU below ob-

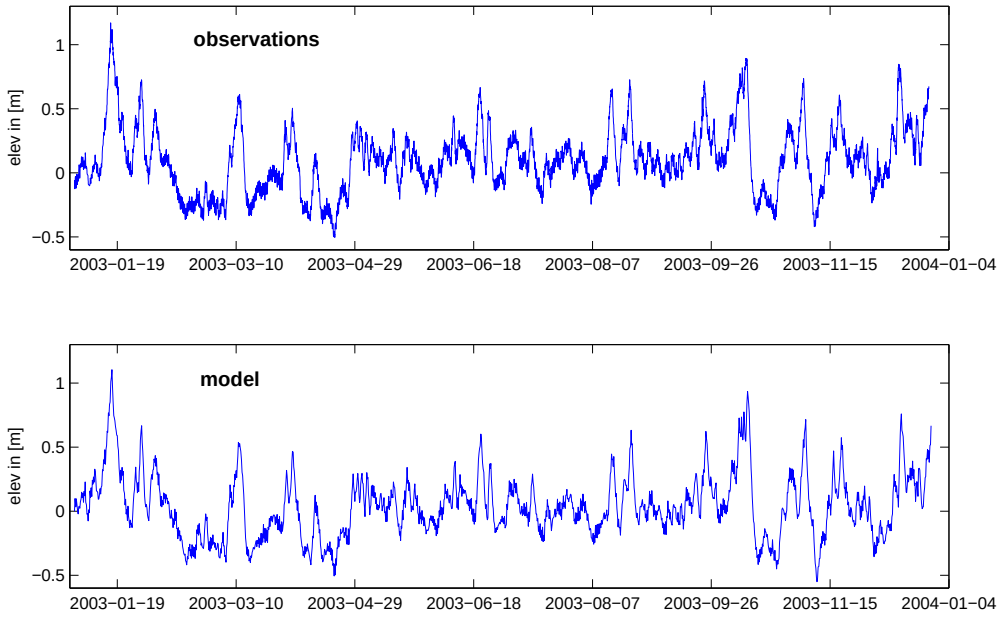

Figure 15: model results and observations of sea surface elevation in Løgstør Bredning

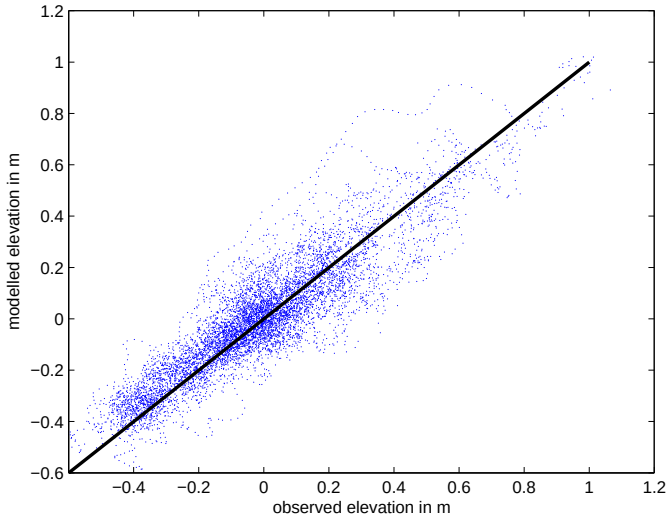

Figure 16: Scatter plot of centred time series of modelled and observed sea surface elevations.

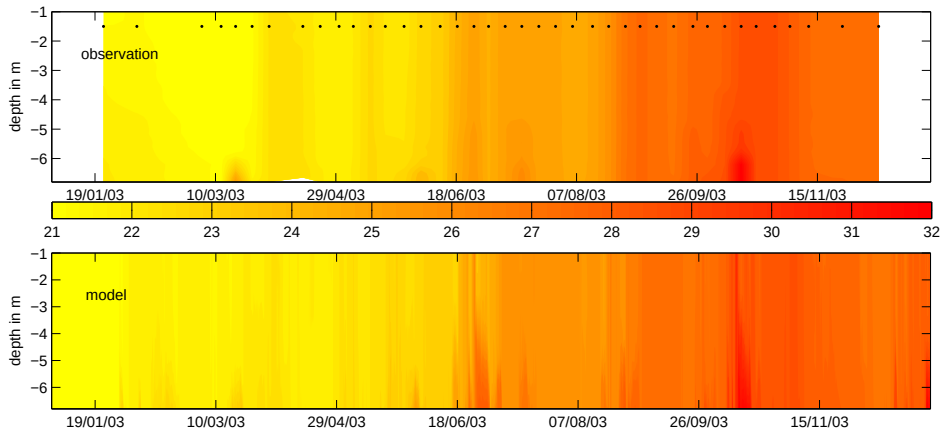

Figure 17: Vertical, modelled and measured salinity profiles for the year 2003 at the monitoring station in Løgstør Bredning.

servation for almost the rest of the year. In the end of December, the differences between the modelled and the observed salinity become smaller. This discrepancy may be due to the discretisation of the bathymetry, or to the lack of evaporation, or to the lack of measurements for the boundary conditions, where the boundary salinity may be underestimated by the linear interpolation (see Figure 7). In August, 2003, measurements and model data show a big inflow event. The Limfjord has some very narrow channels that are discretised by steps of 200m, like the North Sea boundary, Oddesund and Salling Sund. Perhaps some events of the big inflow of August were filtered out by these narrow channels and reduced the intensity of this inflow in August. Another explanation may be the evaporation in the summer months. With evaporation the salinity of evaporated volumes stays in the water column and increases salinity. The rms-differences of modelled salinity and observed salinity for Løgstør Bredning is 0.97 PSU for the salinity at the sea bed and 0.75 PSU at the sea surface. In the area of Thisted Bredning, the model seems to behave more unrealistic than in all other areas having a monitoring station. The differences are not significant in terms of rms-differences, but it seems, that the model does not mirror the events from observations. There are two major problems leading to this lack in the model: First, the initial conditions are at least one PSU too high, so that there is too much salt in Thisted Bredning that has to be mixed out by freshwater or inflow events. But the freshwater input cannot compensate the initial difference at the monitoring point, and the inflow events from the North Sea seem to be filtered out by the narrow channels northwest of the island of Mors. Another problem may be the monitoring point itself. From the end of May until June 2003, it can be seen that there great leaps in salinity of 4 PSU per week up and down. The monitoring point is perhaps located in an area where a salinity front changes its location.

The rms differences in salinity for all monitoring stations are listed in Table 3.

Monitoring Point	rms-difference [PSU] surface salinity	rms-difference [PSU] bed salinity
Løgstør Bredning	0.75	0.97
Nissum Bredning	0.71	1.07
Lovns Bredning	1.47	2.26
Skive Fjord	2.60	1.77
Nibe Bredning	1.34	1.39
Kaas Bredning	1.00	0.85
Thisted Bredning	1.12	1.49
Risgårde Bredning	0.96	1.41

Table 3: rms differences in salinity between the GETM Limfjord Model and the monitoring observations

4.1.3 Temperature

The figures 18 to 25 show graphs of bottom and surface salinity and bottom and surface temperatures. These graphs contain monitoring observations (printed as squares) and model results (printed as lines). In all the figures, the minimum and maximum temperatures of 2003, as they appear in the model, are almost the same as in the observations. At some stations, especially in the shallow parts like Lovns Bredning and Skive Fjord, the temperatures near the sea bed are too high. That is because of the assumption described in 3.6.4. The residual heat at the sea bed heats up only the bottom layer and produces relatively high and unrealistic temperatures in those areas in summer around July and August of 2003, and the same in April and in the end of May. A better implementation of handling residual heat will fix that problem. The residual radiation heats up partially the bottom and leads to a heat flux into the bottom layer. The other part of residual radiation is reflected into the water column again. This process decreases the heating of the bottom layer, but is not included in the GETM Limfjord Model.

The rms-differences in temperatures for all monitoring stations are listed in Table 4.

4.1.4 Velocities

There were velocity observations at the study site in Løgstør Bredning during the MaBenE campaign from the 26 May until the 6 June, 2003. These observations were made in two areas of interest - one over mussel beds and one over sand, being 950 m to the southeast. The water depth at the sandy site was approximately 5 m. For the comparison with modelled velocities the sandy site was chosen, because the

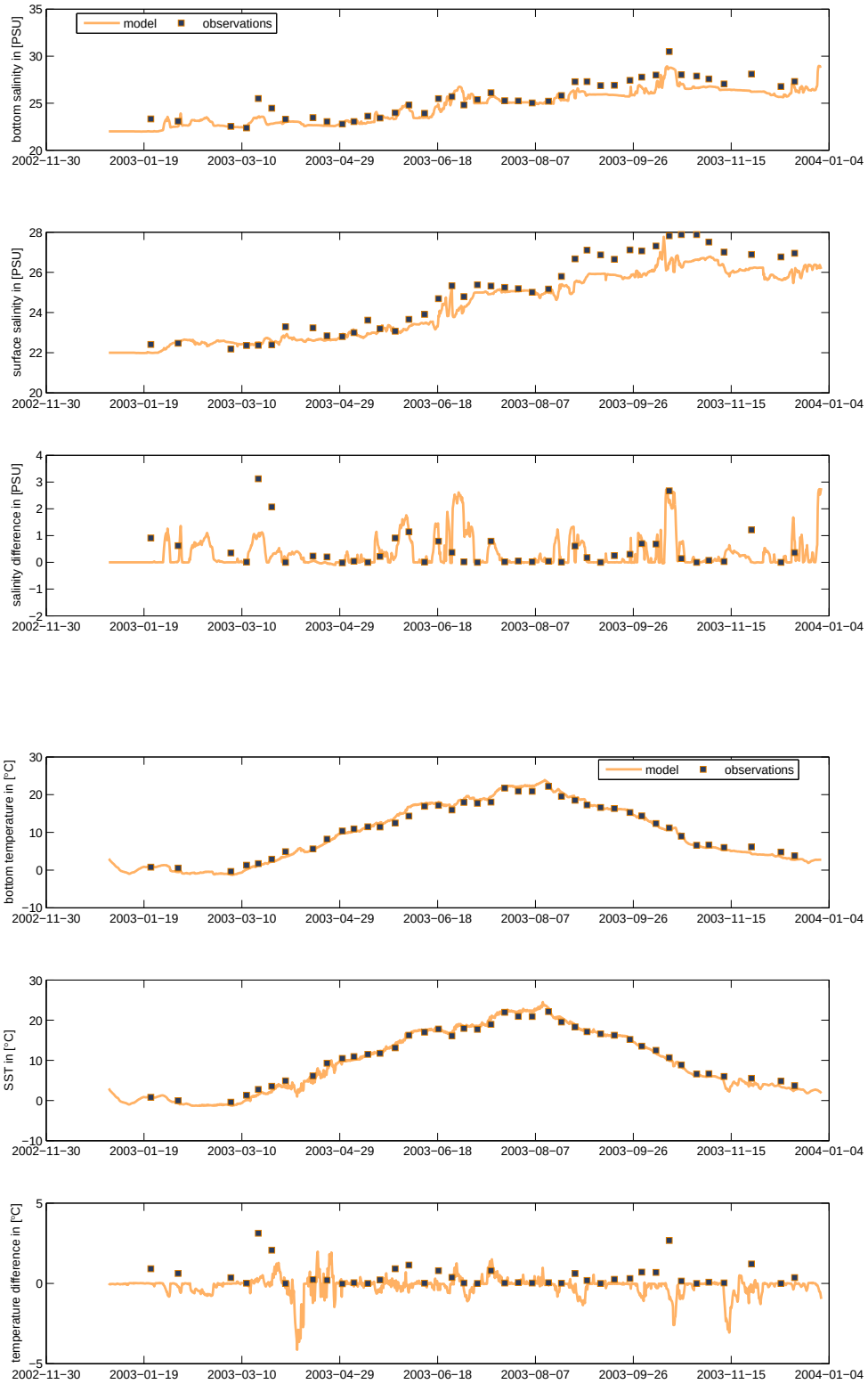

Figure 18: Comparison between modelled salinity and temperature and the monitoring observations in Løgstør Bredning

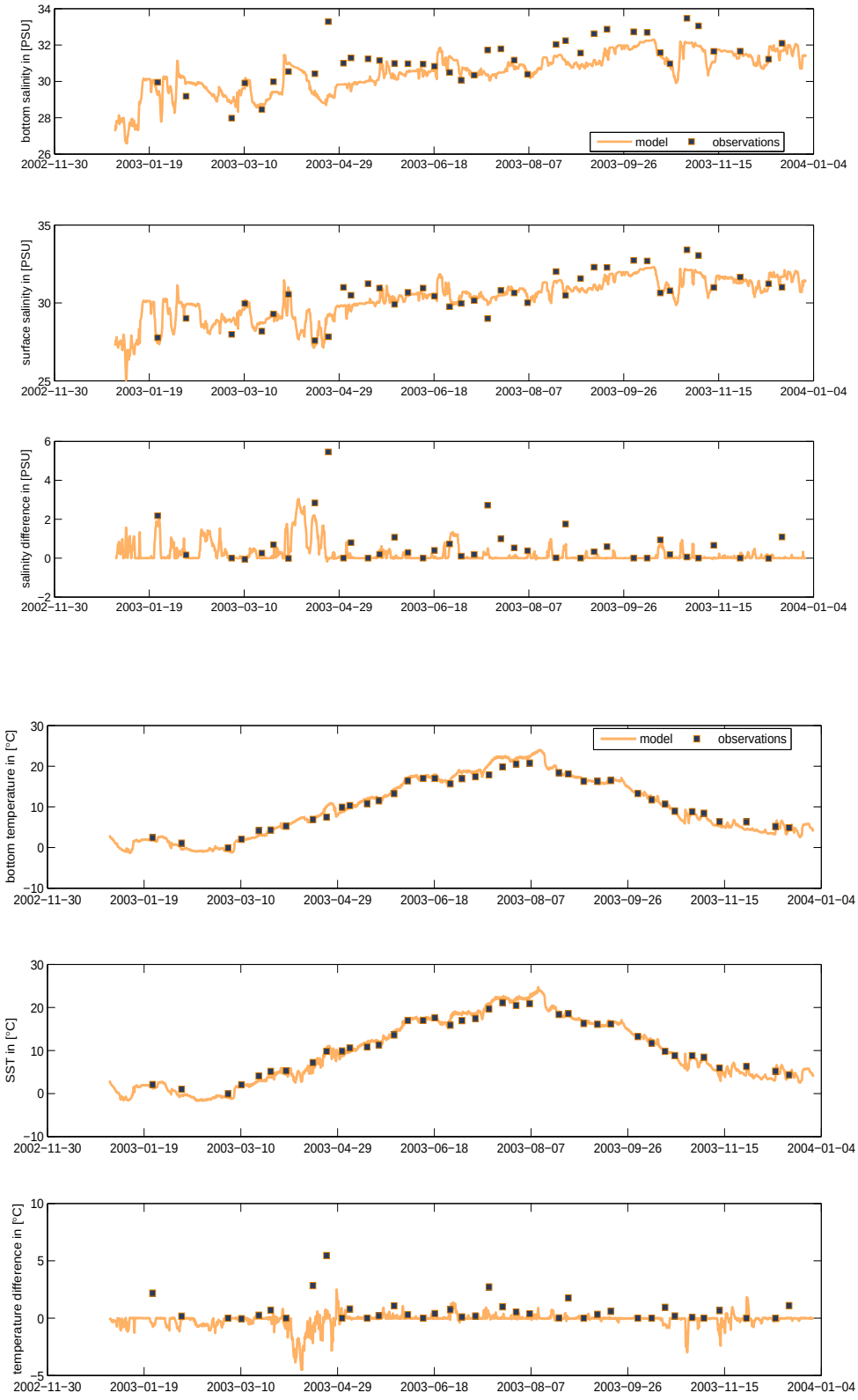

Figure 19: Comparison between modelled salinity and temperature and the monitoring observations in Nissum Bredning

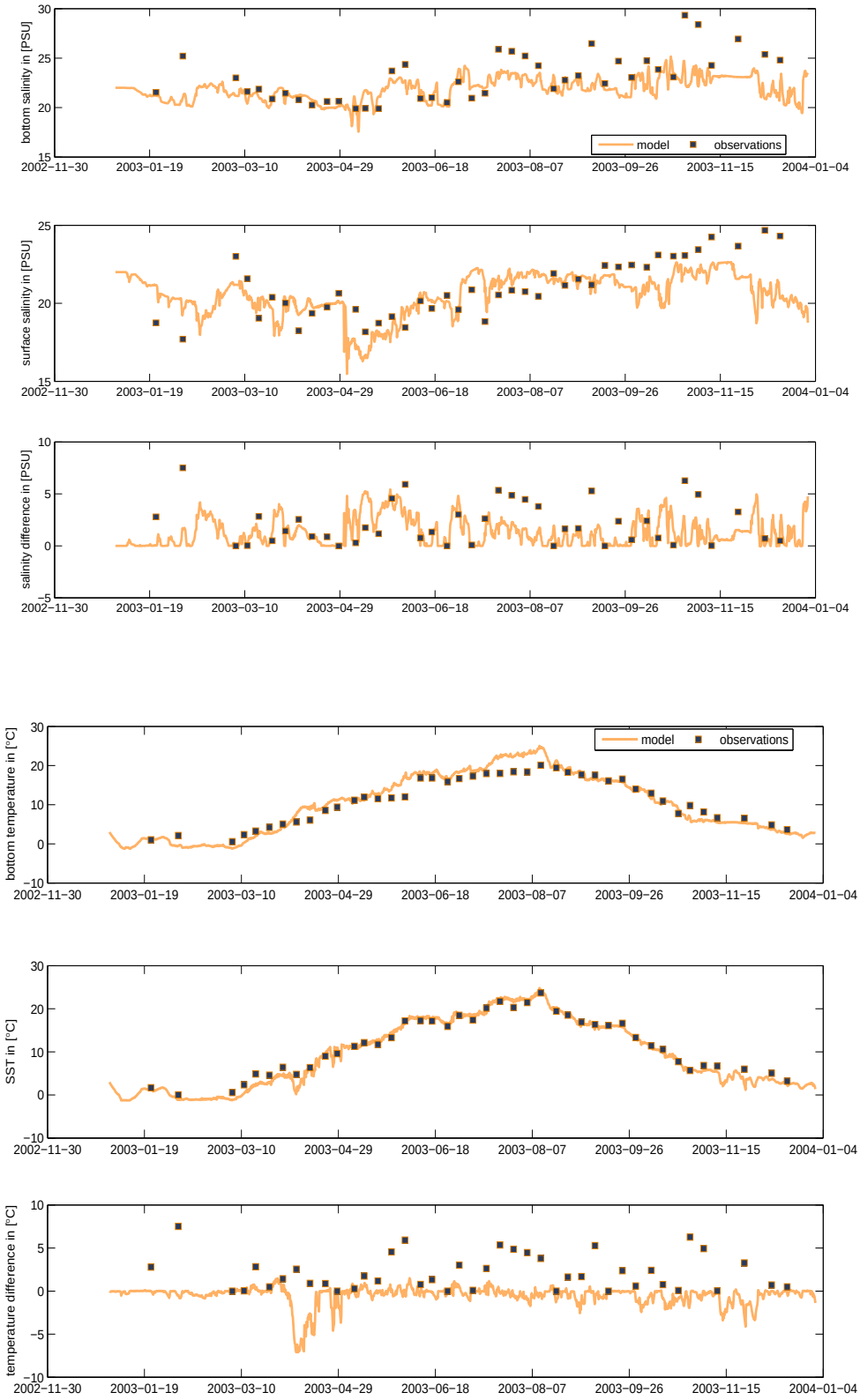

Figure 20: Comparison between modelled salinity and temperature and the monitoring observations in Lovns Bredning

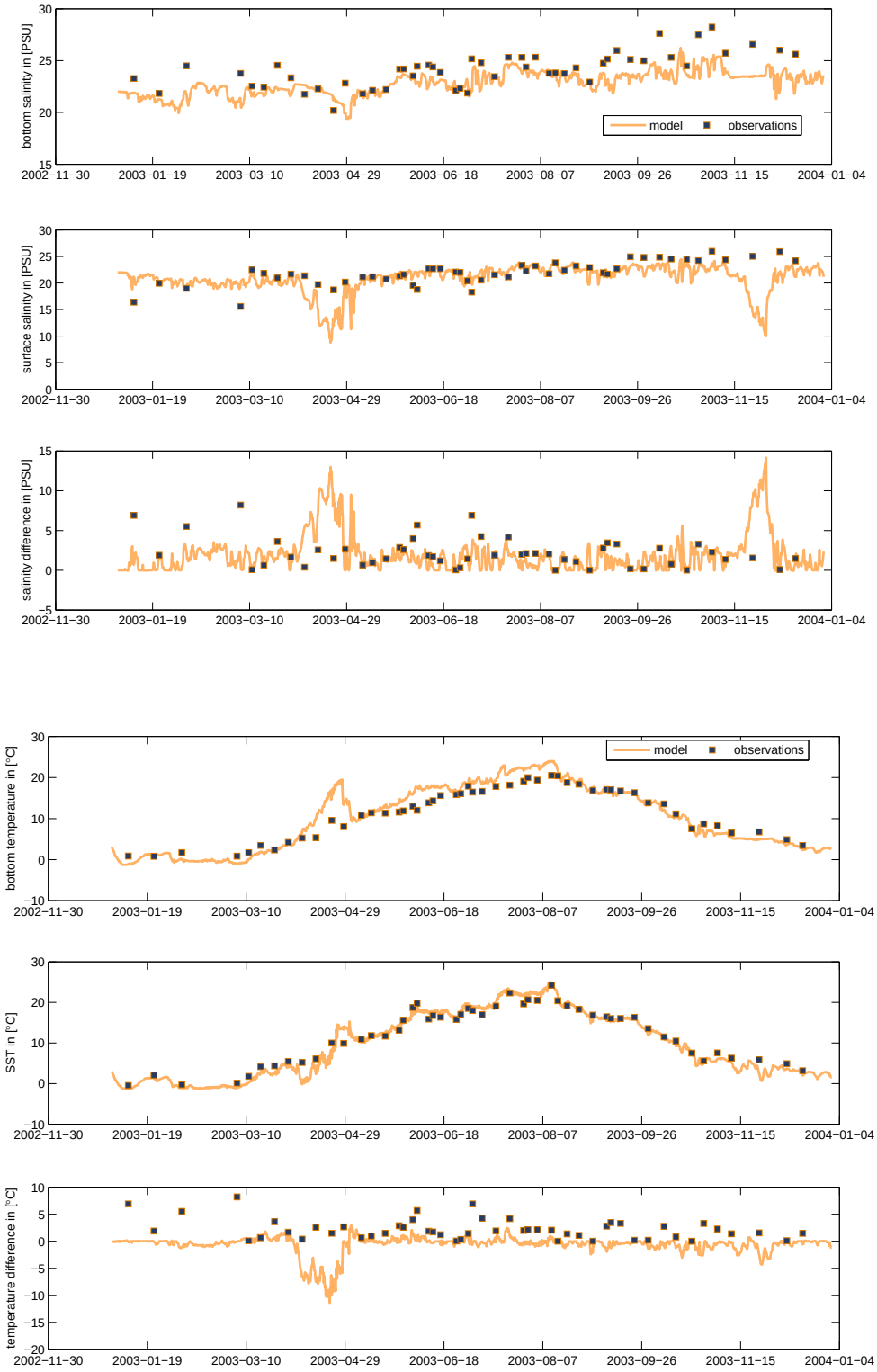

Figure 21: Comparison between modelled salinity and temperature and the monitoring observations in Skive Fjord

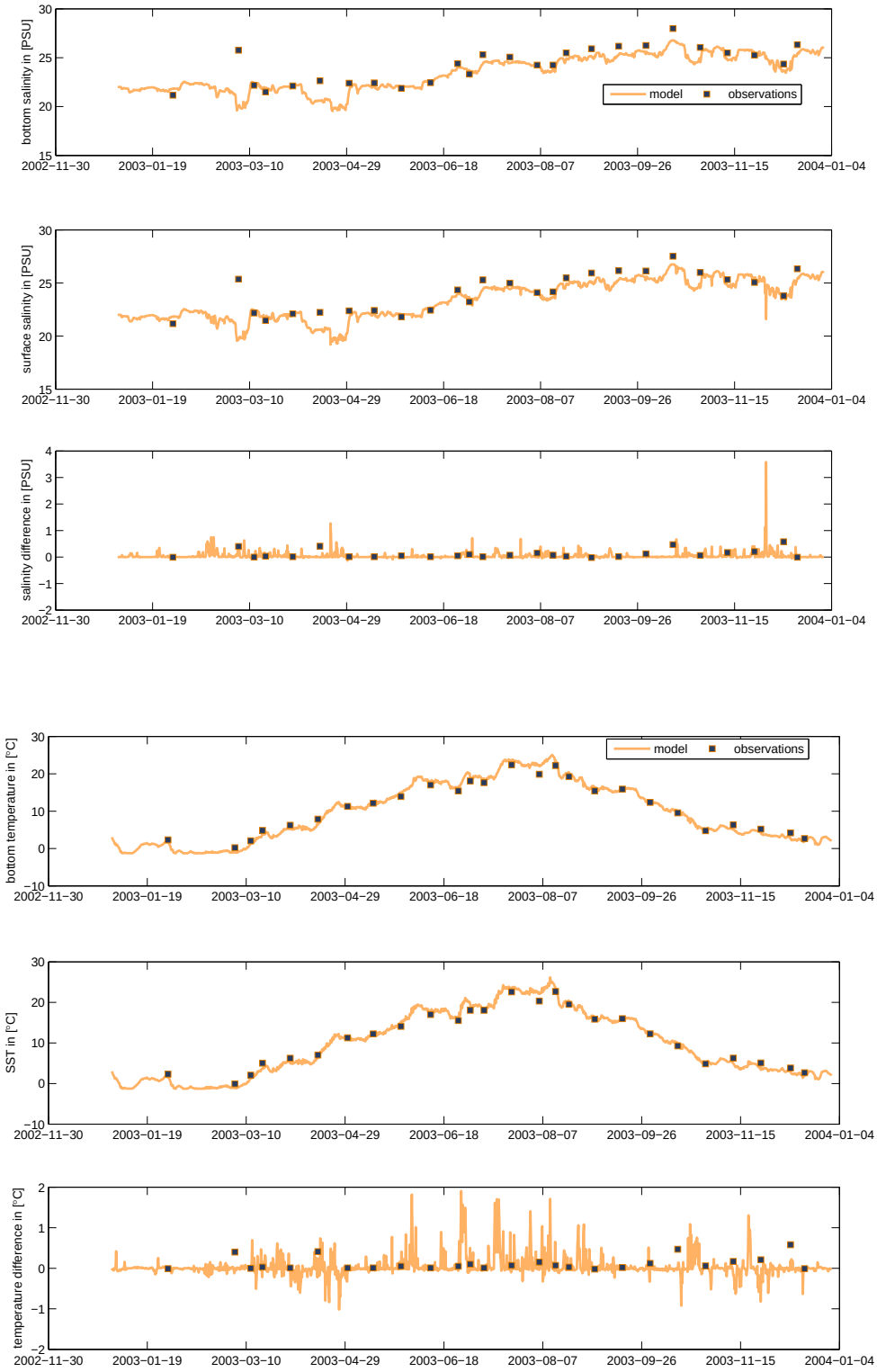

Figure 22: Comparison between modelled salinity and temperature and the monitoring observations in Nibe Bredning

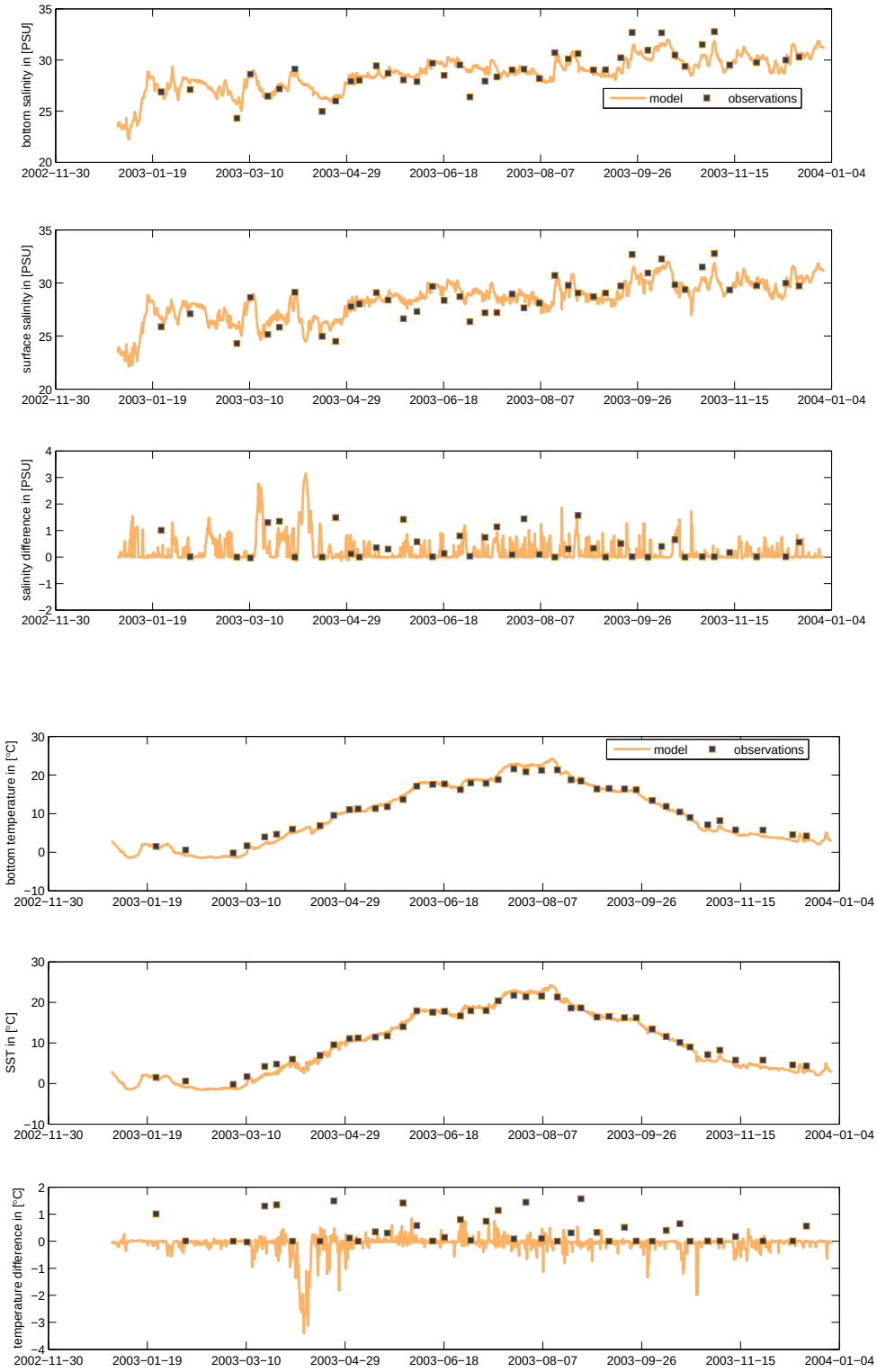

Figure 23: Comparison between modelled salinity and temperature and the monitoring observations in Kaas Bredning

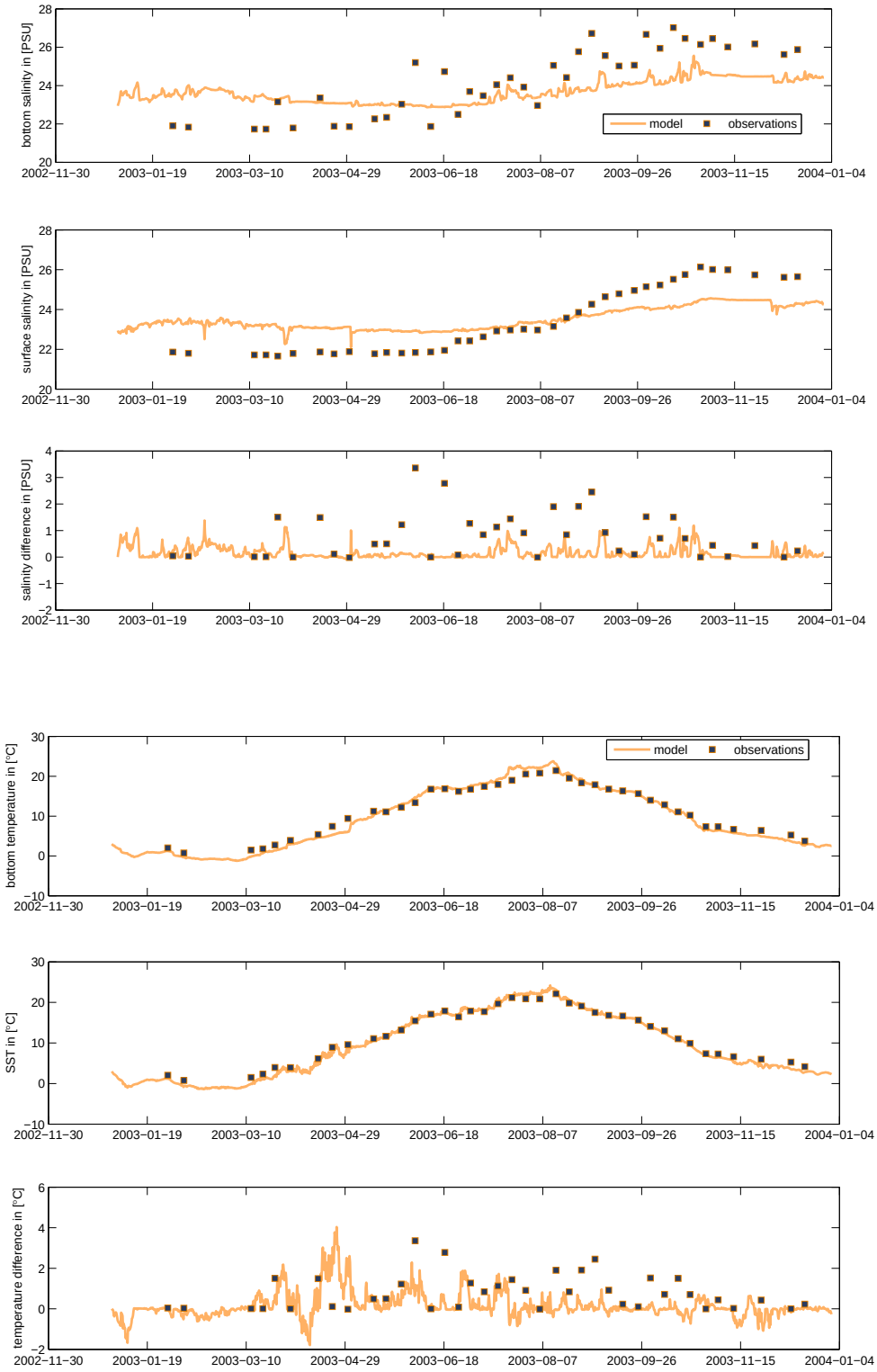

Figure 24: Comparison between modelled salinity and temperature and the monitoring observations in Thisted Bredning

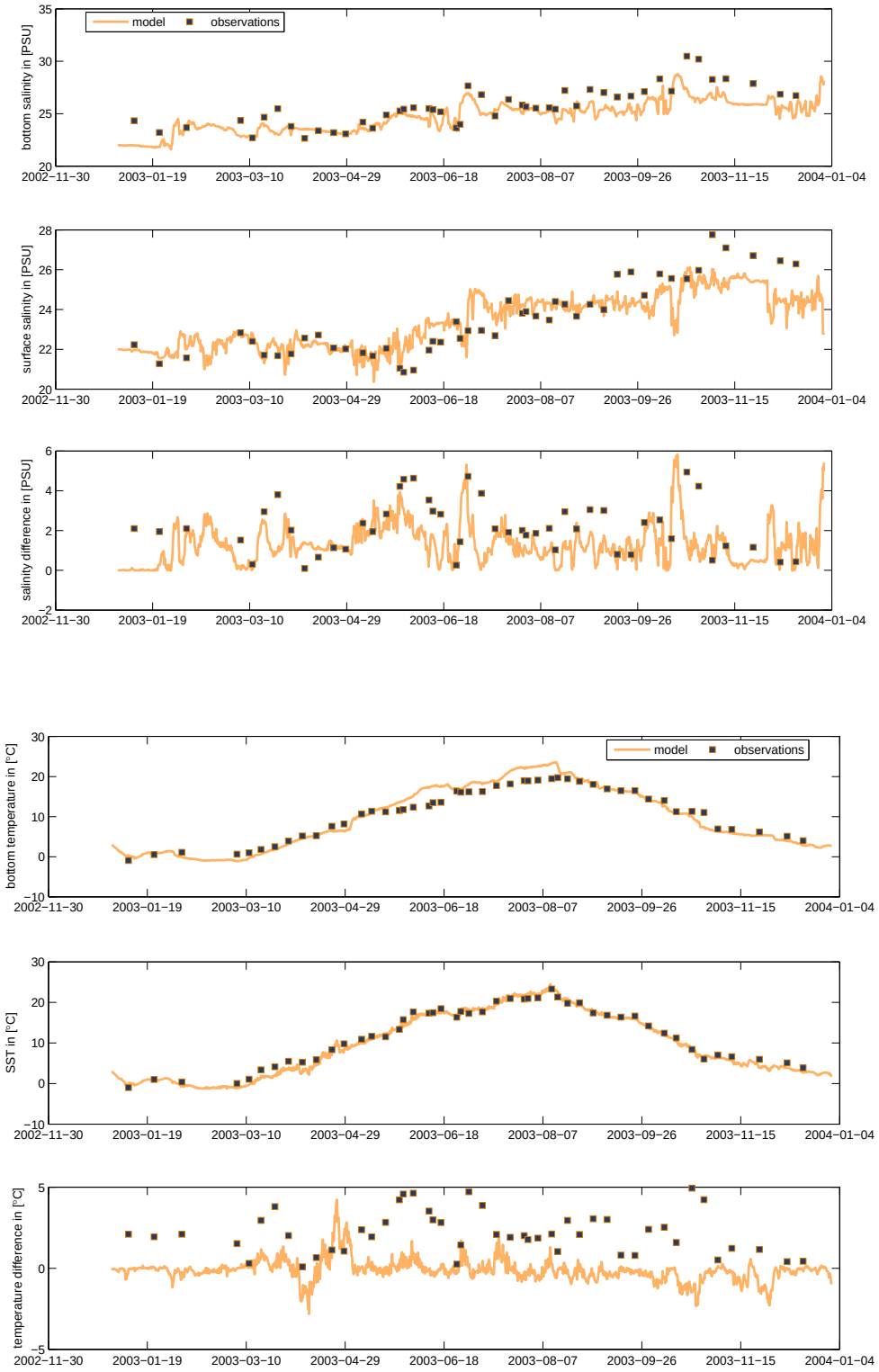

Figure 25: Comparison between modelled salinity and temperature and the monitoring observations in Risgårde Bredning

Monitoring Point	rms-difference [°C] surface temperature	rms-difference [°C] bed temperature
Løgstør Bredning	0.94	0.92
Nissum Bredning	0.92	1.04
Lovns Bredning	1.31	2.08
Skive Fjord	1.61	2.36
Nibe Bredning	0.96	1.07
Kaas Bredning	0.97	0.98
Thisted Bredning	0.93	1.23
Risgårde Bredning	1.04	1.99

Table 4: rms differences in temperature between the GETM Limfjord Model and the monitoring observations

higher roughness at mussel beds was not implemented into the model. A 1200 kHz RDI ADCP was placed by divers at the bed and was "looking" upwards.

ADCP is an abbreviation for Acoustic Doppler Current Profiler. It is an instrument to measure velocities and works like a sonar. At the top of the ADCP, there are four ceramic transducers looking in 4 different, known directions, which are tilted by around 30 degree from the axis of "looking". In general these directions are aligned at 12, 3, 6 and 9 o'clock positions.

For measuring velocities, the ADCP sends a monofrequency signal from its four transducers and switches shortly after this in receiving mode. The sent signal is scattered back to the ADCP by suspended particles and zooplankton, that are moving passively with the flow in the water column. The time shift between sending and receiving a signal gives the distance from the ADCP to the backscattering object and the frequency shift by Doppler effect gives the velocity of the backscattering objects.

In general it is very difficult to compare modelled velocity data on a discrete grid with point measurements. Little differences between the models discrete bathymetry and the always changing real bathymetry will have an effect on modelled velocities directly. Because of this, modelled vertically averaged velocities are compared to the vertical mean of measured velocities. Of course, the ADCP cannot measure velocities in the whole water column, but parts of it at the bed and at the surface are missing. The comparison therefore will show only qualitative similarities and differences. Figure 26 shows the modelled and the measured velocities in eastward and northward direction for the campaign period. The velocities are in both cases very low and compare at least in the order of magnitude. At the observational point, some events that are observed are not resolved in the model. Especially the modelled northward velocity is not very closed to observations. This can be the case, because of inaccurate resolution in space or some local, meteorological events. With the used 1-point meteorological forcing for the whole area, local events are

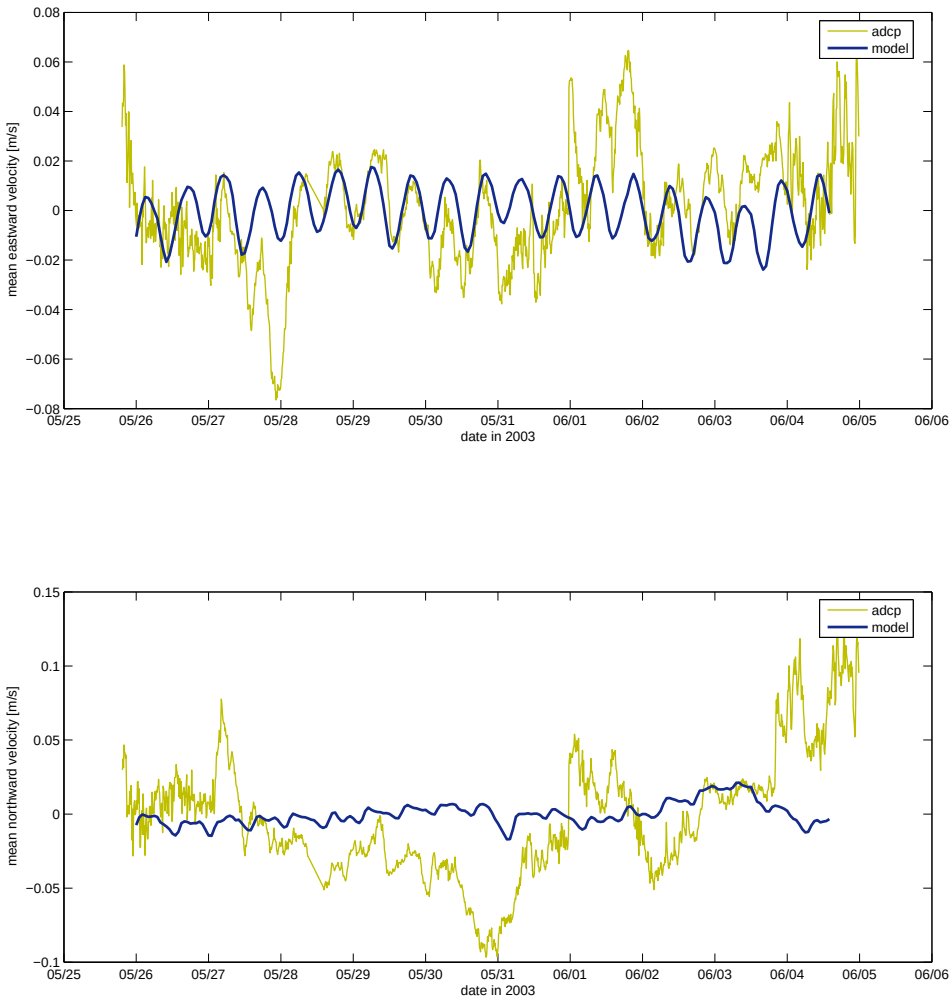

Figure 26: Modelled, vertically integrated northward and eastward velocities compared to the observed velocities for the MaBenE campaign period in 5.8 m depth

not resolved with the model. The effect of a local wind events is reflected in the low flow velocities, because it is not overlayed by a strong mean flow. There is also an insufficiency by the model setup in resolving events with less than 3 hour length of time or less than 6 hour period, because the meteorological forcing changes only every 3 hours. The comparison of eastward velocities shows a good similarity of a tidal signal somehow. It is not a librating change between westward and eastward

flow, its more a tidal driven, periodical eastward flow. The observations show the same signal with almost the same phase and amplitude in periods with low winds (e.g. at May, 28th-30th; see Figure 9).

4.2 T-S analysis for Løgstør Bredning

In Figure 27, the T-S-diagrams for Løgstør Bredning, Skive Fjord and Nissum Bredning are shown, including modelled temperature and salinity data for 2003 of all the 10 vertical levels in the model. The colours of markers in the picture resolve the time with blue being at the beginning of the year and red being at the end of 2003. The T-S-patterns for Nissum Bredning, which is dominated by North Sea water,

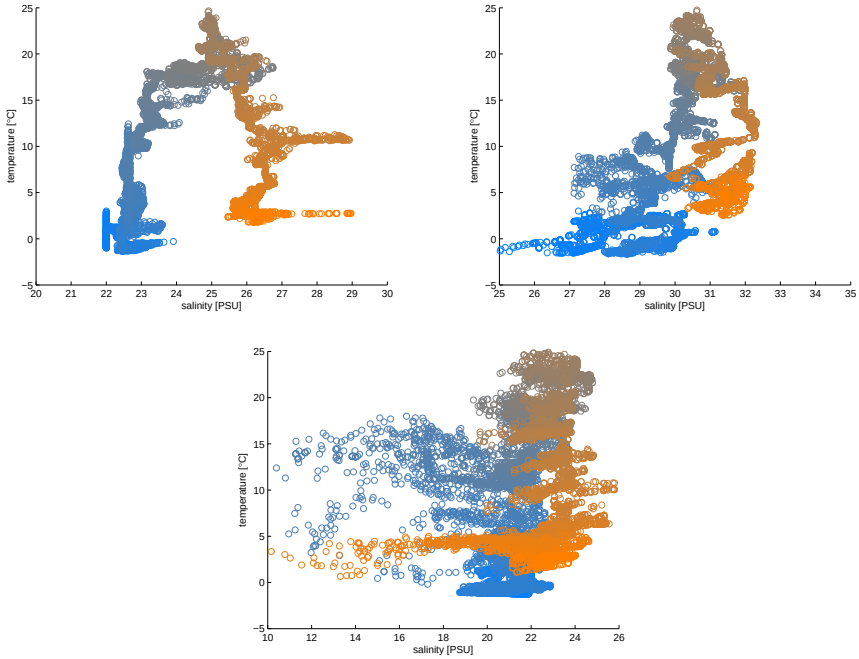

Figure 27: Temperature-Salinity plots for Løgstør Bredning (left), Nissum Bredning (right) and Skive Fjord (bottom) for 2003

and the Skive Fjord, which is dominated by riverine inflows, are closed over the year, so that one can assume an annual cycle of density relevant properties that are annually dominated by temperature. In these shallow waters, the annual temperature variability permeates the whole water column. This ends up in such vertically stretched patterns. The plotted pattern for Løgstør Bredning is not closed as usual for oceanic T-S-diagrams, hence the physical properties of the Limfjord do not only have an annual variability, but a variability over several years. The validation shows that the higher salinity at the end of the year is also measured in the monitoring points. In Figure 28, the T-S-curves of these three typical areas are plotted. Thus it

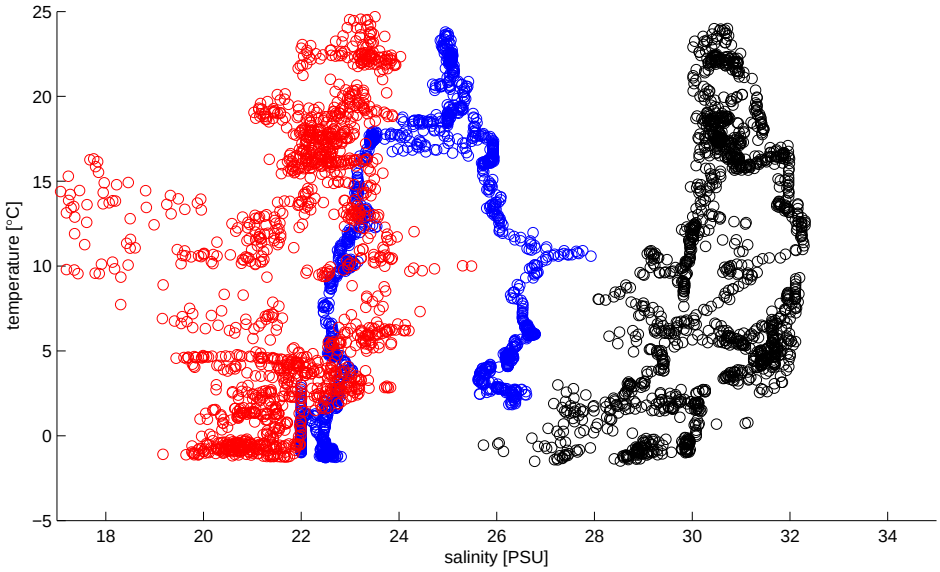

Figure 28: T-S-diagrams for the middle vertical layer in Nissum Bredning (black), Løgstør Bredning (blue) and Skive Fjord (red) for 2003

appears that the water of Løgstør Bredning lies between Nissum Bredning, which is dominated by water of the North Sea, and the Skive Fjord, which is highly influenced by freshwater. In the end of the year, the water type of Løgstør Bredning tends to be more alike the water type of Nissum Bredning water than in the beginning of the year. Hence, Løgstør Bredning is more influenced by water of the North Sea at the end of 2003 than in the beginning of the year, when it was initialised as same water as that of the Skive Fjord.

4.3 Stratification in the GETM Limfjord Model

4.3.1 Stratification in 2003

When looking at the spatial distribution of the modelled anomaly of potential energy ϕ, especially in Løgstør Bredning, one can see that the Limfjord is an area where the whole water body can be fully mixed without stratification and can be stratified in wide areas. Figure 30 shows the anomaly of potential energy for the whole year at the monitoring station in Løgstør Bredning. In Løgstør Bredning, there is no permanent stratification that could lead to permanent oxygen depletion at the bottom for the whole year, but there are times of strong stratification (like in the end of May or the middle of October) and events of causing a lot of vertical mixing, when the anomaly of potential energy decreases suddenly. In the following sections, these events of changes of ϕ are studied. Figure 29 shows the mean potential energy anomaly for 2003, calculated from the model results. Most of the stratification of 2003 occurs in

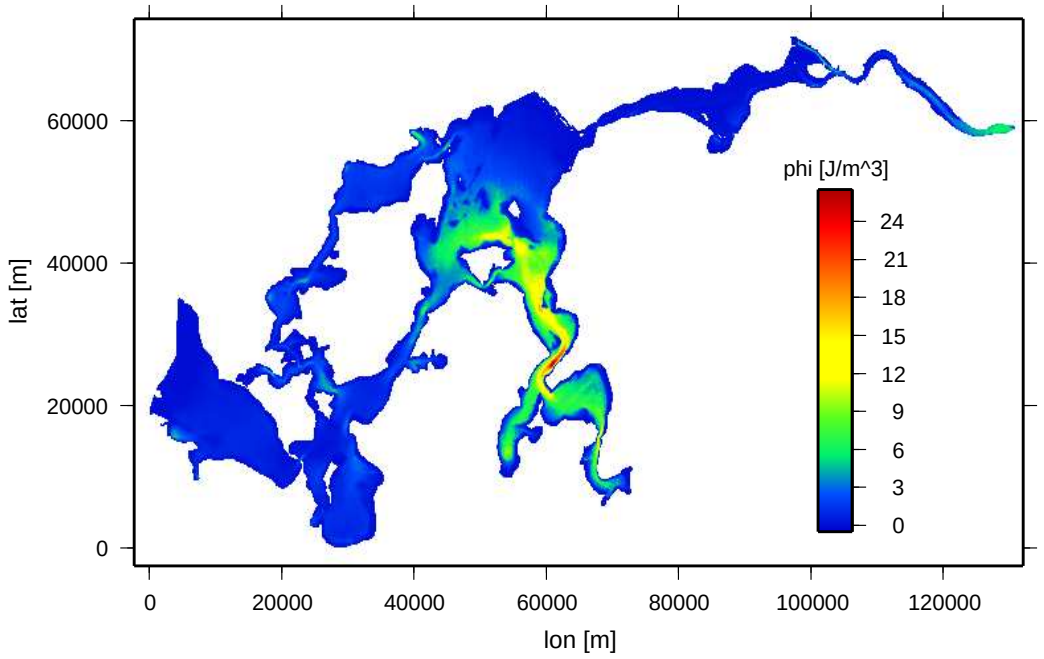

Figure 29: Mean anomaly of the potential energy in 2003 in the GETM Limfjord Model

deep areas like Risgårde Bredning, Hvalpsund and in areas with a lot of freshwater inflow, like in the Lovns Bredning and the Skive Fjord. Strong stratification suppresses mixing and supports stratification in the near future, which should result in a correlation with itself. The period of auto-influence should be much longer than the period of auto-influence of the meteorological forcing. In Figure 31 shows the normalised autocovariance of the anomaly of potential energy. It shows an e-folding time of 3.5 days and a time interval of 10 days until the first zero-crossing. The autocovariance of windspeed out of the meteorological forcing shows a time interval of first zero-crossing of 5 days, which is half the auto-influencing time than of stratification. Stratification influences itself statistically for a period of 10 days until the anomaly of potential energy does not autocorrelate anymore.

The anomaly of potential energy can be influenced by tides, wind, gradients in density, radiation and heat flux. These influences are implemented in the model. Investigations of these influences are shown in the following sections.

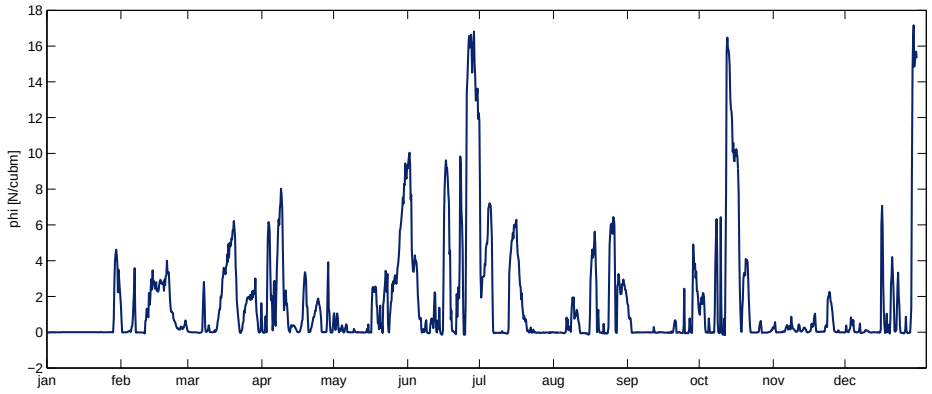

Figure 30: Anomaly of the potential energy in Løgstør Bredning in 2003 from the GETM Limfjord Model

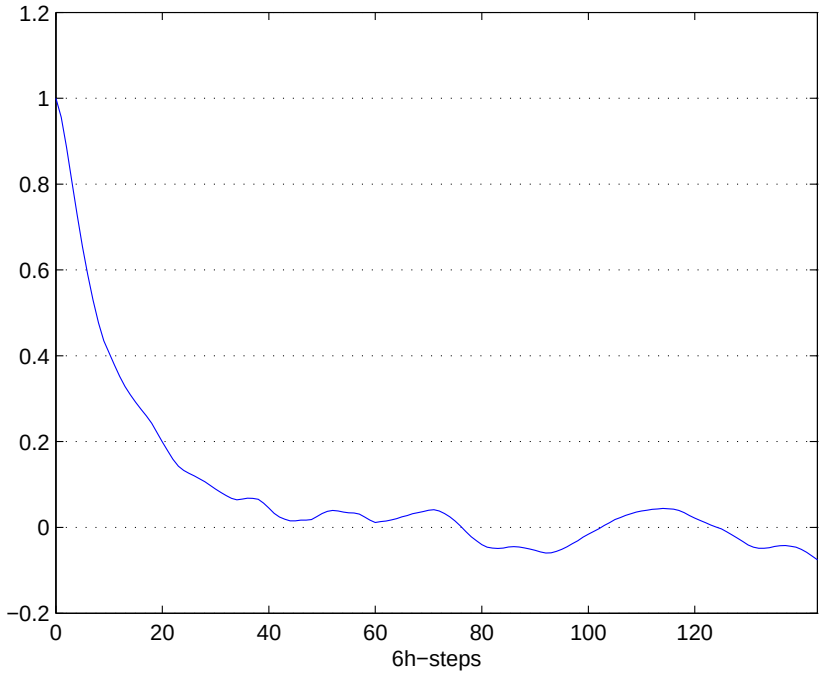

Figure 31: Normalised autocovariance of the anomaly of potential energy for the year 2003 in Løgstør Bredning

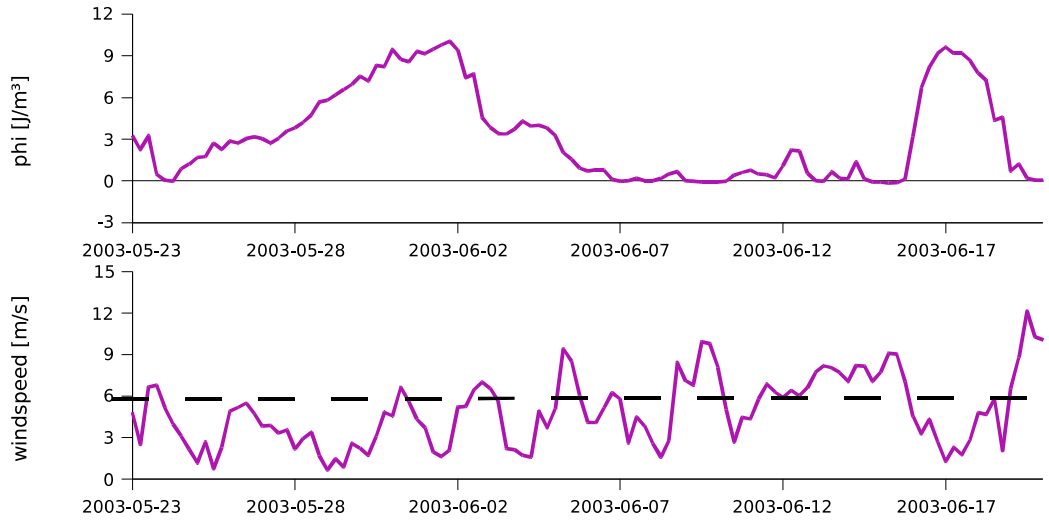

Figure 32: Anomaly of potential energy in Løgstør Bredning for May/June 2003 and wind velocity in 10 m above sea level.

4.3.2 Influences of wind

Wind stirring is an agent acting against stratification. But the turbulence, produced by wind stress, does not mix up the whole water column significantly at every time. The wind has to have a certain minimal velocity to act against stratification. Turbulence produced by light winds does only take place in the upper water column, but not in the deeper parts where the density increases. Figure 32 shows the potential energy anomaly in Løgstør Bredning and the wind velocity. In the graph of wind velocity, a line is plotted at a velocity of 6 m/s. It appears that only winds with a velocity of above 6 m/s have a de-stratifying influence on the water column. Another property of de-stratifying winds is in this picture, that these winds above 6 m/s have to last for at least 12 hours. There is a wind event with a wind speed of above 6 m/s at 31 May, 2003, which lasted only 6 hours. This wind event does not have a significant effect on stratification, see the graph above. On 2 June, wind with a speed more than 6 m/s, lasting for about 18 hours, clearly reduced stratification. Figure 33 illustrates the crosscorrelation of windspeed to the anomaly of potential energy anomaly is shown. The calculated anomaly of potential energy in Løgstør Bredning and the absolute windspeed out of the meteorological forcing, both for the whole year of 2003, were taken as basis. The correlation coefficient of -0.27 is found 6 hours after the wind event set in, which corresponds with the time scale found above where winds have to last at least 6 hours in order to have an effect on ϕ. Figure 33 shows not only a de-stratifying, negative correlation 6 hours after the wind event, but there is also a weak positive correlation 5 days after the wind event. That may come from the stratifying effect of a wind field, when raising the sealevel at the North Sea boundary and causing an inflow. Saline inflows, which produce

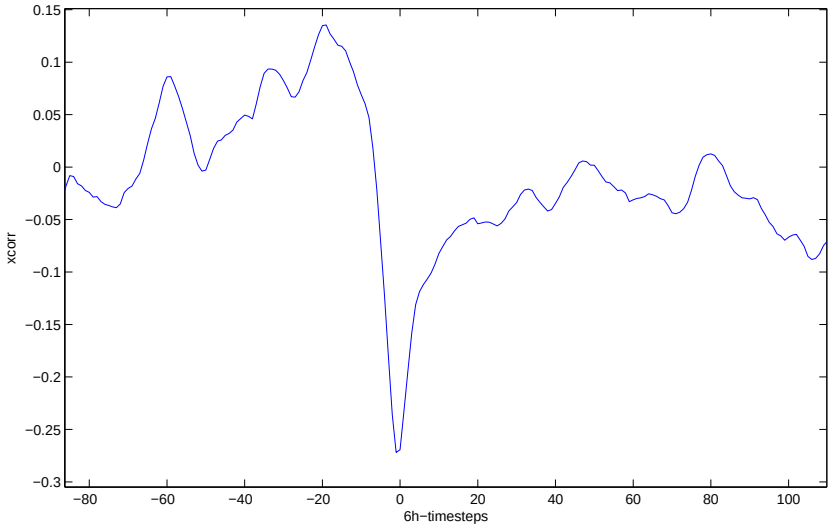

Figure 33: Crosscorrelation of windspeed and stratification ϕ with windspeed being moved by number of 6h-timesteps

stratification in Løgstør Bredning may need 5 days to reach Løgstør Bredning.

4.3.3 Tidal influences

In shelf seas, currents producing turbulence at the bed, thus reducing the stratification, are also driven by tides. In the North Sea and in the Kattegat, there is a clear tidal signal that influences the Limfjord as well. This tidal signal is responsible for a standard deviation in elevation at the North Sea boundary of 0.32 m and at the Kattegat boundary for 0.20 m. These two boundaries are correlated physically, because the tidal wave, which functions as a signal at the North Sea boundary, spreads across the Skargerag into the Kattegat. At the Kattegat boundary, it needs to have a time shift of the size of time, which the tidal wave needs for the distance of $s = 230$ km in waters of $H = 40$ m depth. With the assumption of shallow water waves, this time shift t can be approximated by

$$t = \frac{s}{\sqrt{g \cdot H}}$$

with g being the acceleration of gravity, the time shift thus amounting to 3.2 hours. A cross correlation of the elevations at the North Sea boundary and the Kattegat boundary gives a maximum correlation of 0.78 with a time shift of 6 hours. (see Figure 38 in appendix A.1)

The tidal signal enters the Limfjord and produces tidally generated velocities and elevation patterns. Figure 34 shows the results of a harmonic analysis of hourly

elevation data taken from the model simulation for May 2003. At the top of the plot, the amplitude of M2 tide is plotted for the whole Limfjord. Below, the phase of tidal oscillation is shown and at the bottom of the figure, the mean elevation is shown. To start with the bottom picture, it looks as though the way from Løgstør Bredning to Aggersund, called Løgstør Grunde, acts like a bottleneck for the flow. In May 2003, there was a difference of 6 cm in sea surface elevation over a distance of 8 km. There are other, more narrow channels on the way from the North Sea to the Aggersund, like Oddesund, the channel between Kås Hoved and Jegind Tap or Salling Sund. But these are deep channels of 15-20 m depth. Løgstør Grunde is a very shallow area with a water depth below 1 m and a channel of 400 m width with a depth of more than 4 m. This area determines the throughflow through the Limfjord by bathymetry. When looking at the amplitude of M2 tide, one can estimate the areas that damp out the M2 oscillation. At the North Sea boundary, there is a M2 amplitude of about 26 cm. Within the first 10 km, the amplitude is reduced to the half. The area around the North Sea boundary is characterised by 4 narrow channels, being 4-8 m deep. The next reduction is done by Oddesund, where the M2 amplitudes are reduces from 14 cm to 10 cm. In the area of Tambo Sund, the next reduction of another 4 cm can be seen. In Løgstør Bredning, the M2 amplitude in the model is about 5 cm. From the Kattegat boundary there is a tidal wave coming in with an amplitude of 12 cm. On the way to Løgstør Bredning, there is a slight gradient in the M2 amplitude. It is uncertain, though, wether the tidal signal is being damped out only by bathymetrial influences or by the superposition of tidal waves in the Limfjord. At some places in the Limfjord, it can be observed that M2 amplitudes are annihilated. These amphidromic points are Salling Sund, Visby Bredning and Aggersund. These annihilations are generated by superposition of the incoming tidal waves and the reflected tidal waves. In Lovns Bredning, the M2 amplitude measures 8 cm, which gives an amplification of the tidal wave amplitude of 3 cm compared to the amplitude in Løgstør Bredning. This is due to the combination of bathymetry and wavelength.

One can approximate the tidal stirring in the Limfjord by an term quantifying the energy per volume for reducing stratification, taken from *Simpson and Bowers* [1981]

$$T = \left(\frac{\partial \phi}{\partial t}\right)_{tide} = \frac{4\varepsilon k_b \rho u_s^3}{3\pi H} \tag{21}$$

with ε being the efficiency of tidal stirring, k_b being the seabed drag coefficient, H being the water depth and u_s being the depth averaged amplitude of tidal spring velocities. This tidal stirring term T can be compared to the anomaly of potential energy ϕ from (2.4.6). The ratio ϕ/T gives the time, which the tidal stirring needs for making the water column about fully mixed. When setting $\varepsilon = 0.0037$ (like in *Simpson and Bowers* [1981])), $k_b \approx 0.0025$, $H = 7m$, $u_s \approx 0.1\frac{m}{s}$ and $\rho = 1017\frac{kg}{m^3}$, (21) gives a $T \approx 0.6 \cdot 10^{-6}\frac{W}{m^3}$. With a ϕ of 7.2 $\frac{J}{m^3}$, that means a mid strength stratification in Løgstør Bredning, the tidal stirring would need ≈ 140 days to mix the water column completely.

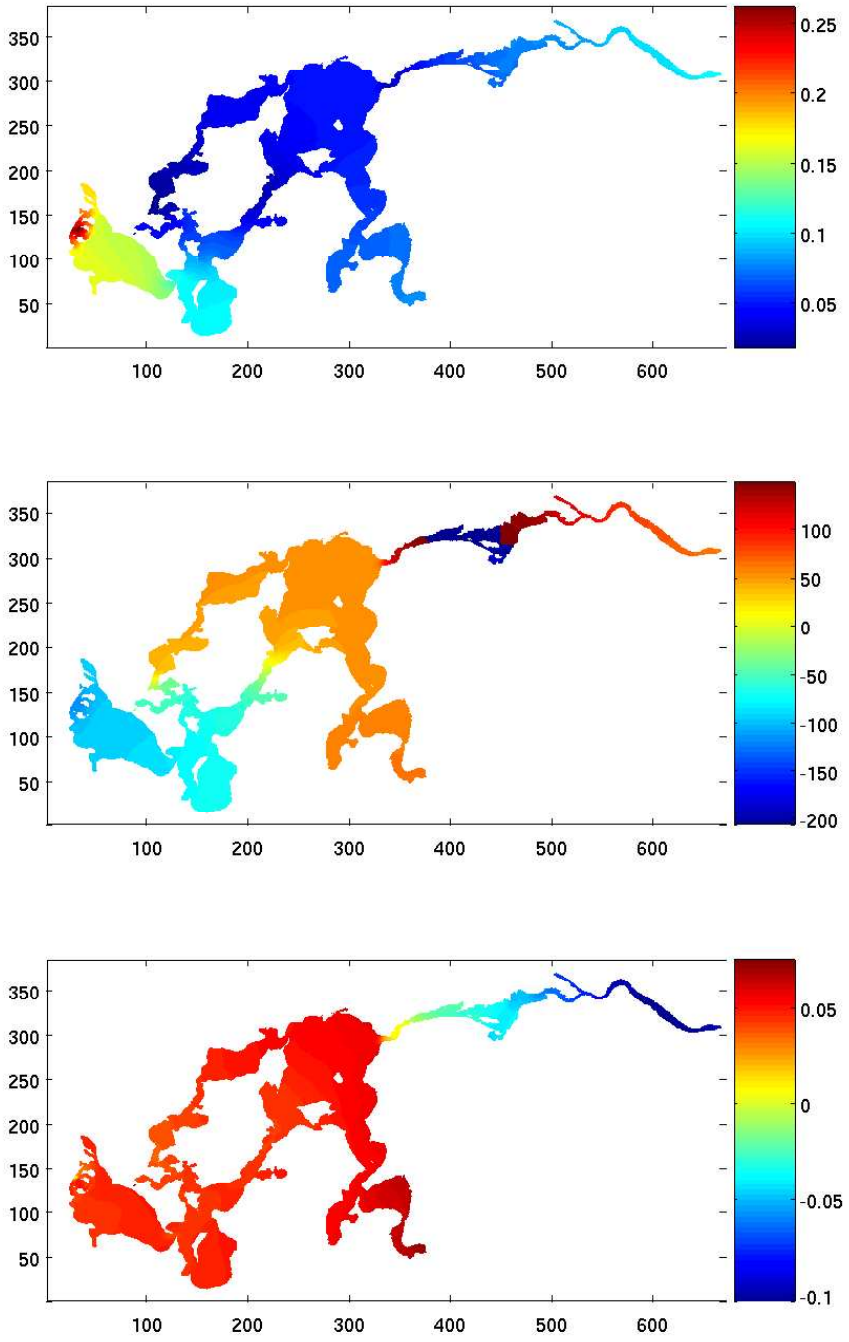

Figure 34: Harmonic analysis for M2-tide of modelled sea surface elevation. Top: amplitude of M2 tide, middle: phase of tidal oscillation, bottom: mean elevation

To conclude, the tidal stirring does not have a significant effect on reducing stratification. The tidal signal is almost filtered out by the narrow and shallow channels and only a weak signal of several centimetres reaches Løgstør Bredning.

4.3.4 Changes in ϕ by heat flux

Local changes of the stratification by heat flux and solar radiation have a stratifying effect in the deep parts of the Limfjord, but for areas like Løgstør Bredning with a water depth below of 10 m, the whole water column is heated up, because the radiation reaches all parts of the water column. In areas where the radiation reaches the sea bed, the water column is heated up from the sea bed with the residual energy from radiation that reaches the sea bed. In this case, the water at the bed gets lighter than the water above and mixing occurs. This de-stratifying effect takes place in areas like northern Løgstør Bredning and Lovns Bredning, for example.

When there is a heat flux into the water column at the surface, the heat flux at the surface and radiation will produce stratification. This process will increase temperatures mainly at the surface and therefore decrease density. This reduction of density at the surface will increase ϕ. When there is heat flux through the surface out of the water column, the temperature decreases at the surface, density increases at the surface and the water column gets instable and ϕ is negative. This instable water column will be mixed up very soon, so there cannot be seen long periods of a negative ϕ when looking at calculations of ϕ out of the model results, for example in Figure 30. In the model, the heat flux through the surface contains the sensible heat flux, driven by the difference between air temperature and temperature of surface water, the latent heat flux, driven by the difference of saturation specific humidity and specific humidity, and long wave back radiation. In terms of ϕ, the change of ϕ by radiation and heat flux can be estimated like in *Wiles et al.* [2006] as follows

$$\left(\frac{\partial \phi}{\partial t}\right)_{heat} = \frac{\alpha g}{2 c_p} \left\{ Q_s (1 - A) T(k, H) - Q_{hf} \right\} \tag{22}$$

with Q_s being the radiation surface flux with an albedo A and $T(k, H)$ being a function of water depth H and the effective diffusive attenuation coefficient for short wave radiation k. $T(k, H)$ is a function determining the effect of heating by remaining radiation at the bottom with the same assumption as in the model implementation (see 3.6.4). For the Limfjord ($H = 7$ m, $k = 0.25$, $a = 0.55$), $T = 0.58$. g is the gravity, α the expansion coefficient, c_p is the heat capacity and Q_u is the upward heat flux, representing the sum of latent heat flux and sensible heat flux out of the water column and the long wave back radiation. In *Wiles et al.* [2006], a typical change in ϕ for a Løgstør Bredning summer regime with a heating rate of $Q_h = Q_s(1 - A)T - Q_u = 160 \frac{W}{m^2}$ contributes a value of $60 \cdot 10^{-6} \frac{W}{m^3}$ to the potential energy anomaly ϕ. A typical mid strength stratification in Løgstør Bredning of 7.2 $\frac{J}{m^3}$ needs about 14 days to improve only by heating.

A crosscorrelation of heat flux out of the water at the surface and the change in potential energy anomaly for the year 2003 at the Løgstør Bredning monitoring sta-

tion gives a maximum correlation coefficient of -0.06. Hence there is no correlation between surface heat flux and stratification in the model. The data used for the correlation had a value every 6 hours. The crosscorrelation of short wave radiation and the change in stratification for the same location and period gives a maximum correlation coefficient of 0.09. Therefore the daily mean change of ϕ and the cumulated daily amount of short wave radiation into the watercolumn was used. Even short wave radiation has not a significant effect on stratification in Løgstør Bredning in the GETM Limfjord Model.

4.3.5 Differential advection

In order to determine the source of stratification in the Limfjord, one idea was to study the differential advection, that means advection that varies with depth. This phenomenon was already characterised in section 2.2 with discussing tidal straining. In the case of tidal straining, the transport of dense water at the surface is greater than the transport of dense water at the bottom, due to bottom roughness. Stratification is produced or destructed by the presence of a horizontal density gradient and shear in currents. In terms of ϕ, we can calculate a $\partial_t \phi(t)$ out of the density advective transport being a function of depth. We can calculate the density advective transport $\tau(z,t)$ by

$$\tau(z,t) = \vec{v}_h(z,t) \cdot \nabla_h \rho(z,t)$$

with $\vec{v}_h(z,t) = \vec{e}_x u(z,t) + \vec{e}_y v(z,t)$ being the horizontal velocity vector and $\nabla_h = \vec{e}_x \partial x + \vec{e}_y \partial_y$ being the horizontal gradient. By calculating a mean advective transport of density by

$$\hat{\tau}(t) = \frac{1}{H} \int_{-H}^{0} \frac{\partial \tau(z,t)}{\partial t} dz$$

and insert $\tau(t)$ and $\hat{\tau}(t)$ into eq. (13), we receive an equation for the change in ϕ by differential advection χ as follows

$$\chi(t) = \frac{1}{H} \int_{-H}^{0} \left(\tau(z,t) - \hat{\tau}(t)\right) g z dz \tag{23}$$

With χ, we have a value for the advective production of anomalies in potential energy, that means a value for the advective production or reduction of stratification.

An estimation of dependencies of χ is not easy because of nonlinearity of stratifying and mixing effects. The forcing for currents in the Limfjord are the horizontal density gradients, generated by inflows from the North Sea against the diffuse freshwater inflow of almost the same magnitude; the mean elevation gradient between the North Sea and the Kattegat, driven by the regional wind field; and the local winds that produce surface currents, but mix the water column as well.

In order to find out the reason for advective production of stratification, four situations are shown in Figure 1. These four situations are some standard situations,

where a special vertical water column is marked as dashed line. This dashed line is the water column of interest in the situations. For each situation, the illustration on the left hand side antecedes the picture on the right. These standard situations A,B,C and D are printed two-dimensionally, but they can be extended to a three-dimensional situation as they can be found in reality. This can be achieved by rotating the figure spirally around the dashed line. This means that the processes, occurring in the horizontal, can be in a different horizontal direction for each depth. Vertical processes do not play a role in these situations of stratifying. A close look at these four situations A,B,C and D reveals that situation B and D are related to each other very closely. The lower vertical half is turned 180 degree around the dashed line. Situation A shows a typical stratifying situation in a tidal regime during ebb tide, as already described in section 2.2. The stratifying conditions are a vertical shear in currents and a horizontal density gradient. Situation B shows a completely different situation of advective stratification. ϕ, or one could say stratification, is advected with a more or less homogeneous current in the whole water column from a stratified water body to the observed water column at the dashed line. Situation C is determined by a vertical current shear and a vertical homogeneous horizontal density gradient like in Situation A. Situation D shows a more typical situation of the Limfjord. There is not a homogeneous vertical density gradient in space, but there is always a density gradient when looking in the directions of currents. With differential advection it is possible to determine the advective production of stratification.

A three-dimensional picture of this situation is shown in Figure 35. In this situation, where the local winds are directed against the direction of an elevation gradient driven or density gradient driven current, a shear in currents is produced. The wind transports freshwater from rivers or less salty water from the Kattegat side into the Limfjord near the surface. At the same moment, a high density inflow in a plume from the North Sea proceeds mainly near the bottom. The salty and denser water slides below the less dense water and stratification is produced.

In section 2.2, estuarine circulation is compared with the lock exchange experiment. The same process is going on in the Limfjord. Without having winds, the internal pressure gradient drives a near-bed flow of saline water into the less saline areas. At the surface an oppositely directed flow of less saline water occurs and the initially mixed system with horizontal density gradients gets stratified. The lifted sea surface elevation in areas where rivers flow into the Limfjord and parallel to the density gradient directed winds at the surface support this mechanism by increasing the pressure gradient near the surface, which drives the less saline flow. Strong winds are responsible for mixing of the Limfjord. The mean horizontal density gradients remain after such a wind event, because of the permanent riverine freshwater input and the permanently high salinity at the North Sea boundary.

In order to find the influence of horizontal advective processes on stratification, $\partial_t \phi$ from the calculated potential energy anomaly at the monitoring station in Løgstør Bredning can be correlated to χ. In order to determine the change in ϕ by differential

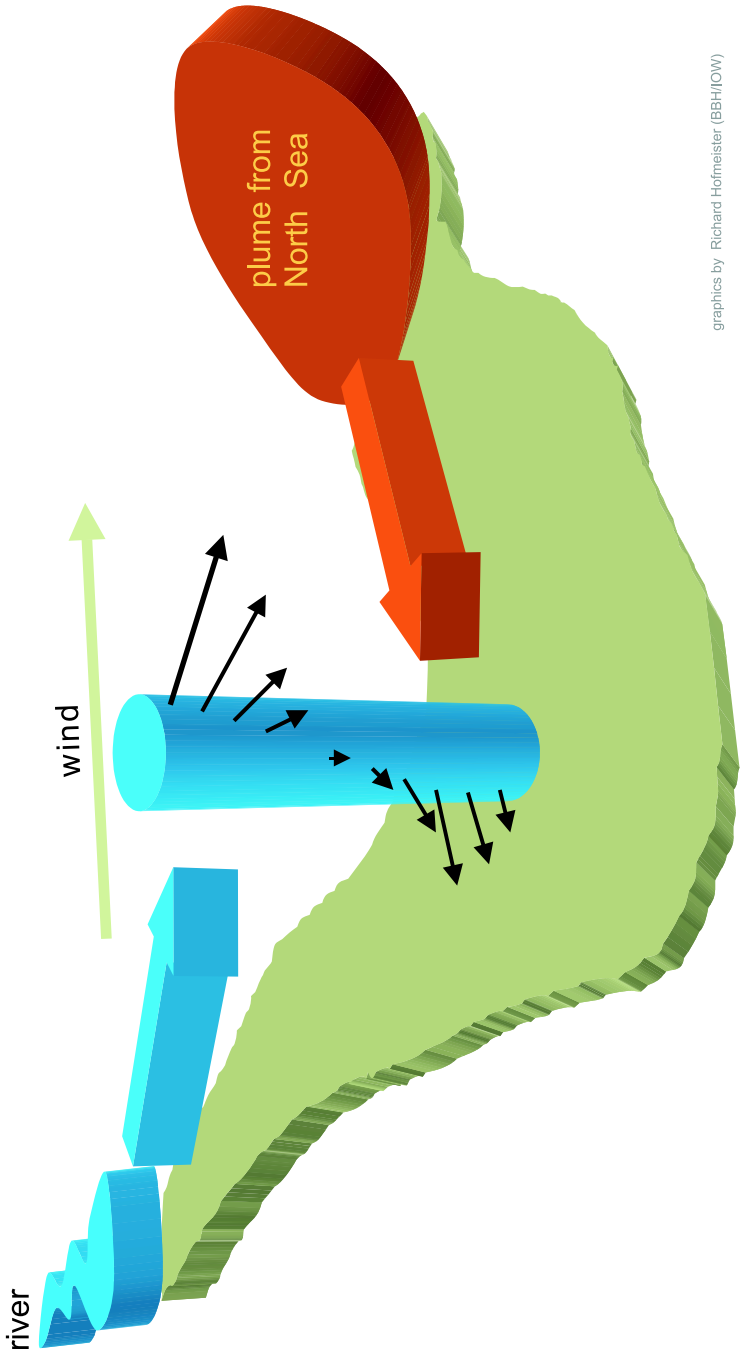

Figure 35: Stratifying situation with differential advection driven by a plume inflow from the North Sea at the bed and a freshwater current driven by local winds at the surface.

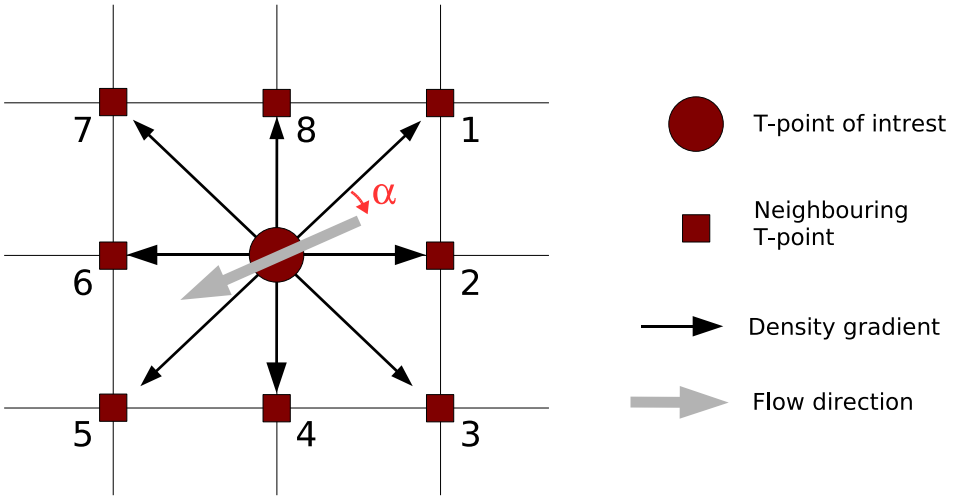

Figure 36: Schematic of how to calculate the density gradient in direction of the flow for one layer

advection after eq. 23, the density gradient in direction of current was calculated for every layer. The values are interpolated linearly with angle between the density gradients to the eight neighbouring water points (see Figure 36) where diagonal neighbours are considered as well, in order to have a continuous range of density gradient. For example: For determining the density gradient for the flow shown in Figure 36 with a grey arrow, the density gradient is linearly interpolated between gradient to neighbour 1 and gradient to neighbour 2 with the ratio of angle α to the angle between direction 1 and 2 (being $\pi/4$). Apparently, there is a relatively high correlation factor of 0.78, which means that the changes in ϕ are mainly a result of differential advection of density, see Figure 37. Advective processes are the determining stratifying agents in the Limfjord. Horizontal differences in heat fluxes are not the main reason for these advective processes. A reduced density by heat flux or radiation at another place in the Limfjord, that influences the observed water column via differential advection, cannot be the reason for an increased differential advection of potential energy anomaly, because the heat flux and radiation from meteorological forcing is the same anywhere in the whole Limfjord. The way to find the reason for the production of stratification by differential advection in the model is to look for sources and sinks for salinity concentration. These are the boundaries where salty water flows into the Limfjord and the rivers. Figure 29 shows that the well mixed regions in the channels to Løgstør Bredning, which lead the saline water from the boundaries with relatively high velocity, did not show a significant mean stratification. But areas with only diminutive flow velocities and riverine freshwater input, show up a tendency to stratification. Especially in areas where the water depth constricts wind mixing to the upper part of the water column and riverine freshwater meets the saline water from the boundaries, a high tendency

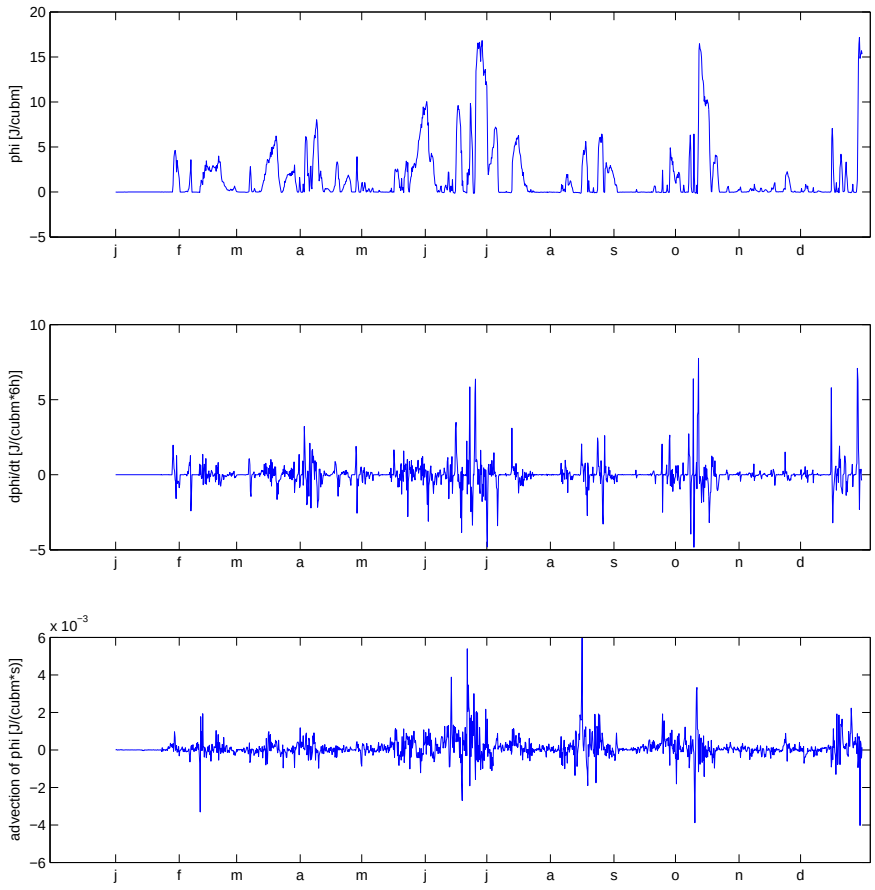

Figure 37: Anomaly of potential energy ϕ in Løgstør Bredning in 2003, $\frac{\partial \phi}{\partial t}$ and the advective change of ϕ

of stratification is found in the model. This is corresponding to the high correlation of stratification with differential advection, because with strong horizontal gradients this can be found in areas with a lot of freshwater input meeting the saline water of the North Sea.

5 Conclusions

During these model studies on stratification in the Limfjord, a realistic, highly resolving 3D model of the Limfjord was developed by means of the circulation model GETM for the year 2003. The model was tuned to give realistic results in Løgstør Bredning, the area of major interest, because the mussels are growing in this area. The validation of the model results with the data from monitoring stations in different places in the Limfjord and data from the MaBenE campaign showed that the model results mirror the observed physical dynamics not only in Løgstør Bredning, but in the whole Limfjord. Some areas beside the main flow in the Limfjord still need some improvement, for example the transport through the narrow channels north of the island of Mors into Thisted Bredning. Furthermore, the assumption on bottom warming without reflection of radiation at the bottom has to be refined in order to obtain a more realistic effect of radiation in the shallow parts of the Limfjord.

The validation showed that the used model, GETM, can reproduce the physical dynamics in estuarine waters like the Limfjord for a simulation period of one year. In the short history of the model GETM and its application for realistic simulations (e.g. *Banas and Hickey* [2005]), the present Limfjord studies show that it is possible to make realistic simulations with the model GETM.

The model results were used to calculate the anomaly of potential energy as quantity describing stratification for the whole Limfjord. In the course of the year 2003, the system of the Limfjord switches between fully mixed and stratified, there is no permanent stratification in the areas where the mussels grow. The model post-predict areas in the Limfjord with high potential for stratification, like Lovns Bredning, Hvalpsund and Risgårde Bredning.

The wind is the major factor of destruction of the stratification in the Limfjord. Winds with at least 6 m/s, lasting at at least 12 hours, reduce stratification in Løgstør Bredning significantly. Statistically, the information about stratification remains in the system of the Limfjord for about 10 days.

The stratifying mechanisms in the GETM Limfjord model is the differential advection. The system of the Limfjord is characterised by strong horizontal salinity gradients between North Sea, Kattegat and the freshwater dominated parts of the Limfjord. The horizontal density gradient drives a stratifying circulation of salty water from the North Sea into the Limfjord at the sea bed under less salty water from the freshwater dominated areas, flowing over the North Sea water at the surface. This mechanism is mainly caused by the internal pressure gradient due to the horizontal density gradients, as well as the difference in mean sea surface elevations at the North Sea boundary and the Kattegat boundary.

The horizontal density gradients in the system of the Limfjord cause a stratifying circulation and strong winds mix the system up from time to time. The horizontal density gradients remain after mixing because of permanent freshwater supply and saline North Sea inflow. These are the major mechanisms at work in the Limfjord which thus switches constantly between stratified and fully mixed.

A Appendix

A.1 Additional Figures

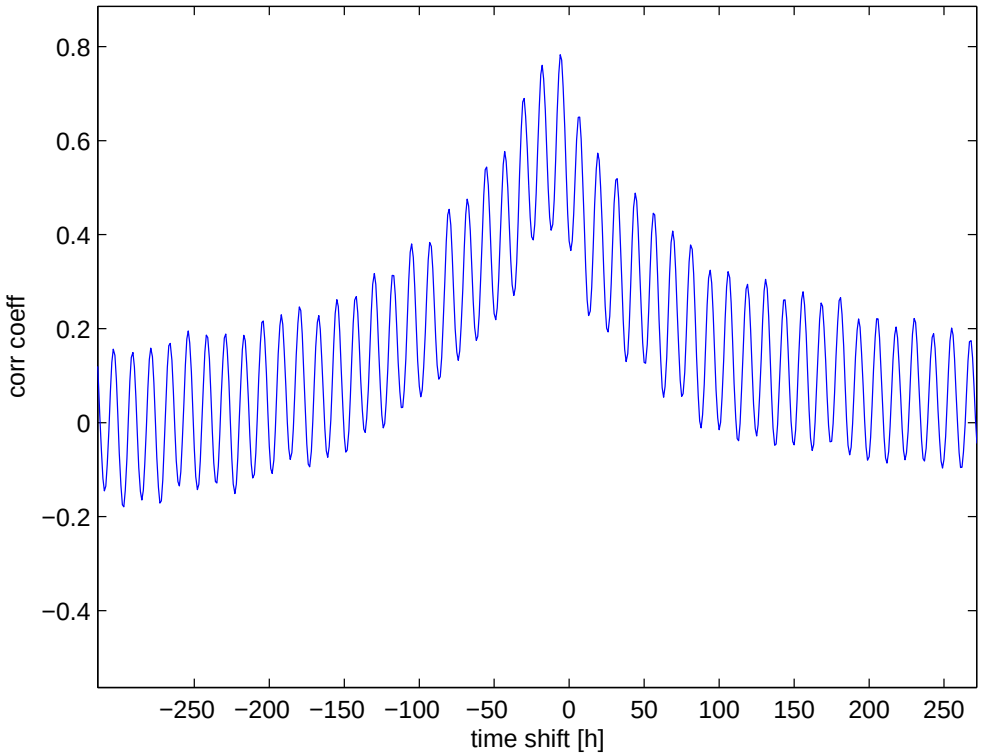

Figure 38: Crosscorrelation of elevations at the North Sea boundary and the Kattegat boundary

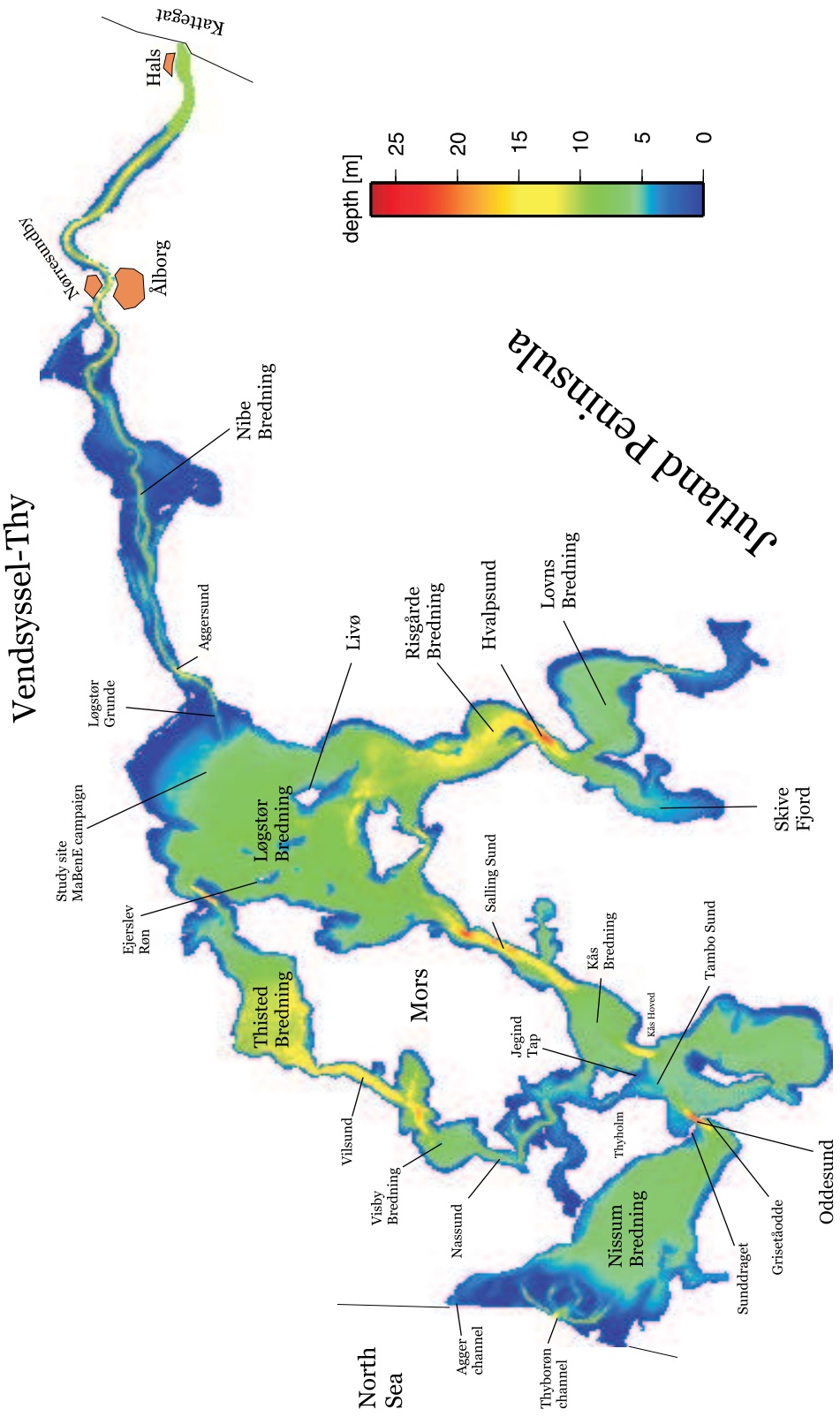

Figure 39: Map of the Limfjord with labels.

List of Figures

References

Ackermann, J., M. Loewen, and P. Hamblin, Benthic-Pelagic coupling over a zebra mussel reef in western Lake Erie, *Limnology and Oceanography*, *46(4)*, 892–904, 2001.

Arakawa, A., and V. R. Lamb, Computational design of the basic dynamical processes of the UCLA General Circulation Model, *Meth. Comput. Phys.*, pp. 173–263, 1977.

Banas, N. S., and B. M. Hickey, Mapping exchange and residence time in a model of Willapa Bay, Washington, a branching, macrotidal estuary, *J. Geophys. Res.*, *110*, C1101, doi:10, 2005.

BSH, Limfjorden, Westlicher Teil, Sea chart 1:130000, 1997.

Buechmann, B., Domain composition, Matlab script, 2004.

Burchard, H., *Applied turbulence modelling in marine waters*, vol. 100 of *Lecture Notes in Earth Sciences*, Springer, Berlin, Heidelberg, New York, 2002.

Burchard, H., and J.-M. Beckers, Non-uniform adaptive vertical grids in one-dimensional numerical ocean models, *Ocean Modelling*, *6*, 51–81, 2004.

Burchard, H., and K. Bolding, GETM – a general estuarine transport model. Scientific documentation, *Tech. Rep. EUR 20253 EN*, European Commission, 2002.

Burchard, H., and O. Petersen, Hybridisation between σ and z coordinates for improving the internal pressure gradient calculation in marine models with steep bottom slopes, *Int. J. Numer. Meth. Fluids*, *25*, 1003–1023, 1997.

Dame, R. F., and T. C. Prins, Bivalve carrying capacity in coastal ecosystems, *Aquatic Ecology*, *31(4)*, 409–421, 1998.

Eriksen, C. C., Measurements and models of fine structure, internal gravity waves, and wave breaking in the deep ocean, *J. Geophys. Res.*, *83*, 2989–3009, 1978.

Frechette, M., and E. Bourget, Food limited growth of *Mytilus edulis L.* in relation to the benthic boundary layer, *Canadian Journal if Fisheries and Aquatic Sciences*, *42(6)*, 1166–1170, 1985.

Freeman, N. G., A. M. Hale, and M. B. Danard, A modified sigma equations' approach to the numerical modeling of Great Lakes hydrodynamics, *J. Geophys. Res.*, *77*, 1050–1060, 1972.

GOTM, General Ocean Turbulence Model, http://www.gotm.net, 2005.

Haidvogel, D. B., and A. Beckmann, *Numerical Ocean Circulation Modelling*, vol. 2 of *Series on Environmental Science and Management*, Imperial College Press, London, 1999.

Jerlov, N. G., *Optical oceanography*, Elsevier, 1968.

Kundu, P. K., *Fluid Mechanics*, Academic Press, 1990.

Martinsen, E. A., and H. Engedal, Implementation and testing of a lateral boundary scheme as an open boundary condition for a barotropic model, *Coastal Engineering*, *11*, 603–637, 1987.

Muschenheim, D. K., and C. R. Newell, Utilization of seston flux over a mussel bed. Marine ecology progress series, *Oldendorf*, *85(1-2)*, 131–136, 1992.

Panofsky, H. A., and J. A. Dutton, *Atmospheric Turbulence*, Wiley, New York, 1984.

Paulson, C. A., and J. J. Simpson, Irradiance measurements in the upper ocean, *J. Phys. Oceanogr.*, *7*, 952–956, 1977.

Phillips, N. A., A coordinate system having some special advantages for numerical forecasting, *J. Meteorol.*, *14*, 184–185, 1957.

Rippeth, T. P., N. R. Fisher, and J. H. Simpson, The Cycle of Turbulent Dissipation in the Presence of Tidal Straining, *J. Phys. Oceanogr.*, *31*, 2458–2471, 2001.

Royal-Frysk, Mytilus edulis, http://www.royal-frysk.de/muschel_d.html, 2006.

Scotti, R. S., and G. M. Corcos, An experiment on the stability of small disturbances in a stratified free shear layer, *J. Fluid Mech.*, *52*, 499–528, 1972.

Simpson, J., and D. Bowers, Models of stratification and frontal movement in shelf seas, *Deep-Sea Research*, *28A*, 727–738, 1981.

Simpson, J., J. Brown, J. Matthews, and G. Allen, Tidal Straining, Density Currents, and Stirring in the Control of Estuarine Stratification, *Estuaries*, *13*, 125–132, 1990.

Sverdrup, H. U., On conditions for the vernal blooming of phytoplankton, *J. du Conseil*, *18*, 287–294, 1953.

Umlauf, L., Turbulence Parameterisation in Hydrobiological Models for Natural Waters, Ph.D. thesis, University of Darmstadt, Germany, 2001, Department of Mechanics, ISBN 3-8311-2627-0.

Umlauf, L., H. Burchard, and K. Bolding, General Ocean Turbulence Model. Source code documentation, *Tech. Rep. 63*, Baltic Sea Research Institute Warnemünde, Warnemünde, Germany, 2005.

Wiles, P., L. van Duren, C. Häse, J. Larsen, and J. Simpson, Stratification and mixing in the Limfjorden in relation to Mussel culture, *J. Mar. Sys.*, *60*, 129–143, 2006.

Danksagung

Ich danke Hans Burchard für die nette Betreuung meiner Arbeit und dafür, dass ich von Bolding & Burchard die Möglichkeiten bekam im Projekt MaBenE mitzuarbeiten. Besonders die Teilnahme an Projektmeetings mit der Möglichkeit einen Vortrag über meine Arbeit zu halten, hat mir einen Einblick in die schönen Seiten des wissenschaftlichen Arbeitslebens erlaubt.

En stork tak går til Karsten Bolding for hans omfattende hjælp med hensyn til parallel-computing, GETM og Linux såvel som hans svar på mine mange e-mails.

Ich danke auch Lars Umlauf und Frank Janssen für die Antworten auf meine Fragen zur Ozeanographie, Modellierung und Matlab. Die allzeit gute Stimmung im gemeinsamen Büro war diesen beiden und Hannes Rennau, meinem Diplomarbeits-Mitstreiter, zu verdanken.

Ich freue mich auf die weitere Zusammenarbeit mit Euch!

Declaration

I hereby declare

- that I have written this thesis without any help from others and without the use of documents and aids other than those stated above,
- that I have mentioned all sources used and that I have cited them correctly according to established academic citation rules,

Rostock, June 8, 2006

. . . . . .
Signature